



Institute for Space Nuclear Power Studies
Department of Chemical and Nuclear Engineering
The University of New Mexico
Albuquerque, New Mexico 87131

Cs-Ba TACITRON: I. EXTINGUISHING CHARACTERISTICS

MOHAMED EL-GENK AND CHRIS MURRAY

FINAL REPORT NO. UNM-ISNPS 1-1992

Subcontract No. S-247-002-001, UES Services Inc., Dayton, Ohio

Performance Period March 1, 1991 - February 12, 1992

19980309 373

March 1992

PLEASE RETURN TO:

**BMD TECHNICAL INFORMATION CENTER
BALLISTIC MISSILE DEFENSE ORGANIZATION
7100 DEFENSE PENTAGON
WASHINGTON D.C. 20301-7100**

DTIC QUALITY IMPROVED 4

U 4385

Accession Number: 4385

Publication Date: Mar 01, 1992

Title: Cs-Ba Tacitron: I. Extinguishing Characteristics

Personal Author: El-Genk, M.; Murray, C.

Corporate Author Or Publisher: Institute for Space Nuclear Power Studies, U. of NM, Albuquerque, NM 8
Report Number: UNM-ISNPS 1-1992

Descriptors, Keywords: Cs-Ba Tacitron Test Facility Modulation Conduction Extinguish

Pages: 00040

Cataloged Date: Mar 18, 1993

Document Type: HC

Number of Copies In Library: 000001

Record ID: 26454



Institute for Space Nuclear Power Studies
Department of Chemical and Nuclear Engineering
The University of New Mexico
Albuquerque, New Mexico 87131

Cs-Ba TACITRON: I. EXTINGUISHING CHARACTERISTICS

MOHAMED EL-GENK AND CHRIS MURRAY

FINAL REPORT NO. UNM-ISNPS 1-1992

Subcontract No. S-247-002-001, UES Services Inc., Dayton, Ohio

Performance Period March 1, 1991 - February 12, 1992

March 1992

TABLE OF CONTENTS

	Page
ABSTRACT	iii
LIST OF FIGURES	iv
LIST OF TABLES	vi
NOMENCLATURE	vii
1. INTRODUCTION	1
1.1 Motivation	1
1.2 Extinguishing Mechanisms.....	2
2. DESCRIPTION OF CS-BA TACITRON TEST FACILITY	4
3. OPERATION CHARACTERISTICS	7
3.1 Current Modulation Timing Characteristics	10
3.2 Extinguishing and Ignition Characteristics	10
3.2.1 Establishing of Equilibrium Condition	15
3.3 Conditions for Stable Modulation	17
3.4 Forward Conduction Voltage Drop.....	19
4. DISCUSSION AND ANALYSIS OF EXTINGUISHING RESULTS	26
4.1 Unstable Modulation Regime	27
4.2 Ignition Characteristics During Stable Modulation	30
4.3 Effect of Grid Potential on the Anode Delay-time	33
5. SUMMARY AND CONCLUSIONS	37
ACKNOWLEDGEMENTS	38
REFERENCES	39

Cs-Ba Tacitron: I. Extinguishing Characteristics

ABSTRACT

The extinguishing characteristics of a Cs-Ba tacitron as a switch/inverter are investigated experimentally in three modes of operation: breakdown mode, I-V mode, and current modulation mode. Operation parameters measured include switching frequency up to 8 kHz, hold-off voltage up to 180 V, current densities in excess of 15 A/cm^2 , switch power density of 1 kW/cm^2 , voltage drop as low as 1.5 volts, for a switching efficiency in excess of 94% at collector voltages greater than 30 V. The voltage drop during both the I-V and current modulation modes strongly depend on the Cs pressure and to a lesser extent on the emission properties of the emitter (i.e. emitter temperature and Ba pressure). Increasing the Cs pressure and/or the emission current decreases the voltage drop in the triode sections. However, for the same initial Cs pressure and emission conditions, the voltage drop in the I-V mode is usually lower than that during current modulation.

Results show that at an initial Cs pressure of 20 mtorr, Ba pressure of 0.1 mtorr, and emitter temperature of 1400 °C, the voltage drop in the triode section in the I-V mode could be as low as 1.5 V. At the same operation condition during stable current modulation, so long as the discharge current is kept lower than the emission current, the voltage drop could be as low as 3 V. The Cs pressure, Ba pressure and emitter temperature influence not only the voltage drop but also the stable current modulation of the device (i.e. ignition and extinguishing of the discharge occur when positive and negative pulses are applied to the grid, respectively). Results show that in order for stable modulation to occur the initial amount of Cs atoms in the discharge volume at the time of ignition should be sufficiently high, however, in order to successfully extinguish the device, the heavy components in the discharge volume should be sufficiently low. Therefore, for a given discharge current there is a narrow range of Cs pressures at which stable current modulation is possible. However, for a given Cs pressure and discharge current the on-time and off-time need to be sufficiently long. The former allows the concentration of heavy components to become low enough for extinguishing to occur, and the latter allows the Cs atoms in the discharge volume to replenish so that the discharge can be ignited.

LIST OF FIGURES

	<u>Page</u>
Figure 1. A Schematic Cross-Section of the Cs-Ba Tacitron.....	5
Figure 2. Typical Operation Characteristics of the Cs-Ba Tacitron in the Breakdown Mode.....	8
Figure 3. Current Modulation Timing Diagram for the Cs-Ba Tacitron.....	9
Figure 4. Extinguishing and Ignition Characteristics of the Cs-Ba Tacitron During Stable Current Modulation at 5 kHz ($T_E=1233$ °C, $T_C=583$ °C, $T_g=585$ °C, $T_{Cs}=151$ °C, $T_{Ba}=530$ °C)	11
Figure 5. Voltage-Current Characteristics of the Cs-Ba Tacitron During Extinguishing Phase of Stable Modulation at 5 kHz.....	13
Figure 6. Typical Characteristics During Unstable Current Modulation of the Cs-Ba Tacitron.....	14
Figure 7. Duty Cycle as a Function of the Positive Grid Potential for Various Operating Parameters.....	18
Figure 8. Time Response of the Discharge Current and Forward Voltage Drop Showing the Effect of the Emission Current at $T_{Ba}=500$ °C ($P_{Ba}=0.02$ mtorr) and $T_{Cs}=150$ °C ($P_{Cs}=8.5$ mtorr); (a) $T_E=1200$ °C, (b) $T_E=1250$ °C, (c) $T_E=1300$ °C, (d) $T_E=1350$ °C, and (e) $T_E=1400$ °C	20
Figure 9. Time Response of the Discharge Current and Forward Voltage Drop Showing the Effect of the Emission Current at $T_{Ba}=550$ °C ($P_{Ba}=0.1$ mtorr) and $T_{Cs}=150$ °C ($P_{Cs}=8.5$ mtorr); (a) $T_E=1200$ °C, (b) $T_E=1250$ °C, (c) $T_E=1300$ °C, (d) $T_E=1350$ °C, and (e) $T_E=1400$ °C	21
Figure 10. Time Response of the Discharge Current and Forward Voltage Drop Showing the Effect of the Emission Current at $T_{Ba}=550$ °C ($P_{Ba}=0.1$ mtorr) and $T_{Cs}=170$ °C ($P_{Cs}=21.4$ mtorr); (a) $T_E=1200$ °C, (b) $T_E=1250$ °C, (c) $T_E=1300$ °C, (d) $T_E=1350$ °C, and (e) $T_E=1400$ °C.....	22
Figure 11. Effect of T_E/T_{Ba} ratio on the Discharge Current and Forward Voltage Drop of the Cs-Ba Tacitron, (a) forward voltage drop, (b) discharge current.....	25
Figure 12. Discharge Current, Forward Voltage Drop and Ion Current to the Grid Illustrating Time to Reach Equilibrium During the Discharge	28
Figure 13. Discharge Current and Forward Voltage Drop Showing Time to Reach Equilibrium in the Breakdown Mode.....	31
Figure 14. Stable Modulation of the Cs-Ba Tacitron Showing the Anode Delay-time for a Positive Grid Voltage of 22 V.....	32

	Page
Figure 15. Time Dependent Voltage and Current Characteristics of the Cs-Ba Tacitron During Stable Modulation at \sim 5 kHz and Positive Grid Potential of 22 V; (a) collector and grid current, (b) I-V characteristics. Operation conditions are the same as figure 14.....	34
Figure 16. Effect of Increasing the Positive Grid Potential to 30 V on the Anode Delay-time During Stable Current Modulation	35
Figure 17. Effect of Increasing the Positive Grid Potential to 30 V on the Anode Delay-time During Stable Current Modulation	36

LIST OF TABLES

	<u>Page</u>
Table 1. Tacitron Physical Dimensions	6

NOMENCLATURE

τ_m	: Modulation period of tacitron (s)	T_E	: Emitter temperature (K)
τ_{off}	: Off-time of discharge (s)	T_C	: Collector temperature (K)
τ_{rise}	: Rise-time of discharge (s)	T_g	: Grid temperature (K)
τ_{on}	: On-time of discharge (s)	T_{Cs}	: Cesium reservoir temperature (K)
τ_{fall}	: Fall-time of discharge (s)	T_{Ba}	: Barium reservoir temperature (K)
τ_{ad}	: Anode delay-time (s)	T_a	: Arithmetic average of the emitter and collector temperatures (K)
τ_g	: Pulse width of negative grid voltage (s)	T_f	: Basis flange temperature (K)
$\tau_{g\text{-max}}$: Pulse width of maximum negative grid voltage (s)	T_e	: Electron temperature (K)
τ_g	: Applied grid period (s)	P_{Cs}	: Cs reservoir vapor pressure (torr)
V_{ce}	: Applied voltage between collector and emitter (V)	P_{Ba}	: Ba reservoir vapor pressure (torr)
V_d	: Voltage drop between collector and emitter (V)	P_a	: Cs vapor pressure in the gap (torr)
V_{g+}	: Applied positive grid voltage (V)	M_a	: Mass of Cs atom (kg)
V_{g-}	: Applied negative grid voltage (V)	M_i	: Mass of Cs ion (kg)
I_c	: Discharge current to collector (A)	m_e	: Mass of an electron (kg)
I_g	: Grid current (A)	Γ_i^{mean}	: mean ion flux leaving the gap
k	: Boltzmann's constant (J/K)	Γ_a	: atom flux into the gap, $1/4 n_a \bar{v}_a$
q	: Electron charge (C)	\bar{v}_a	: mean atom velocity
S	: Area through which ions leave the gap into surrounding regions (0.54 cm^2)	ΔN_a	: total amount of atoms leaving gap during τ_{eq}
		f_m	: Modulation frequency of tacitron, $(1/\tau_m)$, (Hz)
		f_g	: Applied modulation frequency to grid, $(1/\tau_g)$, (Hz)
		η_s	: Switching efficiency, $\{(V_{ce}-V_d)/V_{ce}\}$, (%)
		η_d	: Duty cycle, $\{(\tau_g-\tau_{off})/\tau_g\}$, (%)

1. INTRODUCTION

The earliest work on the Cs-Ba tacitron has been published in 1972 in the former Soviet Union.^{1-4,13,14} Although the performance of the Cs-Ba tacitron as a high temperature switch/inverter is expected to be significantly better than other devices, such as the hydrogen tacitron, understanding the physical processes occurring in the Cs-Ba interelectrode gap during various operation modes, and the ignition and extinguishing characteristics of the device is needed. An experimental test facility is established at the University of New Mexico's Institute for Space Nuclear Power Studies (ISNPS), in collaboration with Kurchatov Institute of Atomic Energy (KIAE) in Moscow, Russia, to investigate the performance and further develop the technology of the Cs-Ba tacitron as a switch/inverter for space applications¹⁻⁴. The operation of the Cs-Ba tacitron is investigated in three modes: (a) breakdown mode, (b) I-V mode, and (c) current modulation mode. The breakdown mode is used to test the voltage hold-off capabilities of the tacitron. The I-V characteristics are measured and used to determine the switching efficiency, defined as the ratio of the voltage drop in the interelectrode gap to the hold-off voltage of the device. In the current modulation mode, the capability of the tacitron to generate AC power is investigated. The grid potentials for the turn-on and turn-off of the device as well as the values of the Cs pressure and emission conditions (Ba pressure and emitter temperature) for stable current modulation are investigated experimentally.

1.1 Motivation

Space nuclear power systems are being designed to supply low voltage/high current DC electrical power in the range of a few tens to hundreds of kilowatts to support a host of civilian and military missions. The output power of these systems is preconditioned to a low voltage/high current AC signal using Solid-State Inverters (SSI). Although these inverters have high switching efficiencies (>98%) and are relatively light weight, they are vulnerable to high temperatures (>500 K) and to nuclear radiation. High temperatures cause material loss by sublimation, hence shortening the lifetime of SSIs. In addition, high fluxes of fast neutrons and gamma rays cause

malfunctions of the SSI due to single and multiple event upsets. In case of minor upsets the recovery time of SSI is very long, on the order of milliseconds. Both shielding and separation distance from nuclear reactors are used to provide a tolerable radiation environment at a mass penalty. Therefore, it is desirable to develop inverters that are compatible with high temperature and nuclear radiation environments, have a relatively low mass, a high efficiency, a high modulation frequency, and a long operation lifetime.

A Cs-Ba vapor Thermionic (TI) inverter/switch called "tacitron" could satisfy all the requirements listed above. It is essentially a thermionic converter with a third electrode (grid) that switches the device "on" and "off". The tacitron employs a low pressure cesium and barium vapor mixture (pressure $\sim 10^{-3}$ torr) in the interelectrode gap and has a large gap size (~ 4.25 mm); hence, precluding a possibility of a gap closure and short circuiting the electrodes. The Cs vapor neutralizes the space charge in the interelectrode gap, while the Ba vapor, adsorbed onto the surface of the electrodes, lowers the work function and increases the emission current density. Because thermal and/or radiation exposure are unlikely to degrade operation, the tacitron is inherently thermal and radiation hard.

1.2 Extinguishing Mechanisms

The spontaneous and controllable current interruption of grid-controlled switching devices filled with Cs-Ba vapor mixtures has been previously studied by Kaibyshev *et al.*,¹ Kaibyshev and Kuzin,² and then Kaplan *et al.*⁵ It was shown that the discharge current can be interrupted spontaneously when it reaches a critical value. A similar behavior has been observed earlier in the discharges using mercury vapor. Several hypothesis have been suggested in the past to explain this phenomena, which include: (1) a reduction in the neutral gas density at high current densities, which leads to the formation of a charged double sheath at constrictions in the discharge channel, such as a grid aperture,^{6,7} (2) a pronounced inhomogeneity within the grid control elements in the discharge volume,⁸ and (3) a depletion of neutrals due to the removal of ions when the plasma is highly ionized.^{2,9-11}

At high current densities, the plasma in the Cs-Ba tacitron could be highly ionized; therefore, most of the heavy components are ions.^{2,12,13} During the conduction state of the device, the leakage of ions to the surrounding reduces the concentration of heavy components in the gap, which under certain conditions causes the discharge process to become unstable and self-extinguish. The conditions for such an interruption to occur in the Cs-Ba tacitron are high discharge current, that is high emission from the emitter, and low Cs pressure. High discharge current can be obtained reliably during the long lifetime of the device by the addition of Barium vapor, which provides high emission currents at a low vapor pressure (10^{-4} torr).

The instabilities in the Cs-Ba tacitron leading to successful current interruption (discharge extinguishing) depend on the discharge current and the Cs vapor pressure in the interelectrode gap. At the onset of discharge, ions are swept from the discharge region lowering the Cs atom density in the gap. An instability will occur if the discharge current is above a critical value determined by plasma conditions (or the amount of heavy components in the discharge volume is sufficiently low). This phenomenon eventually causes the discharge in the Cs-Ba tacitron to self-extinguish. If the ionization fraction is high, an instability can be elicited by applying a negative potential to the grid. In this case, in order to successfully extinguish the device, the discharge (on-time) should be sufficiently long, which affects the switching frequency of the tacitron.

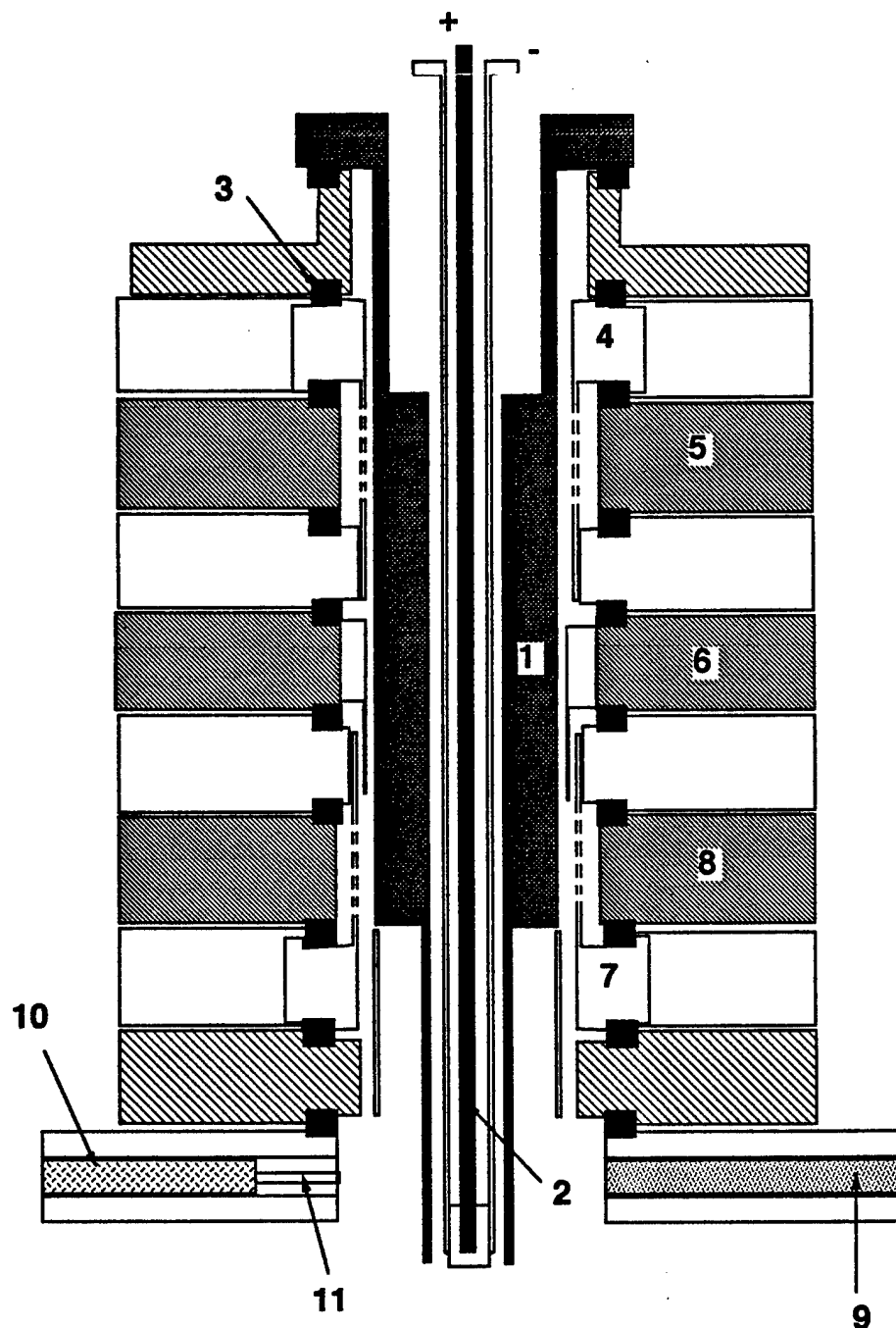
Another factor which affects the switching frequency of the Cs-Ba tacitron during stable current modulation, is the off-time needed to replenish the Cs atoms into the interelectrode gap after the discharge has been extinguished¹⁵. As discussed earlier, during the on-state of the device, the concentrations of Cs atoms and ions in the gap decrease, and under certain conditions the Cs atoms would not be replenished during the off-time to the value necessary to ignite the discharge when a positive pulse is applied to the grid.^{12,13} Subsequently, discharge ignition would not occur; the ignition voltage depends strongly on both the length of the off-time and the P_{ad} parameter.^{15,16} For more details on the dependence of discharge ignition on Cs pressure and emission conditions see reference (15).

2. DESCRIPTION OF CS-BA TACITRON TEST FACILITY

The Cs-Ba tacitron test facility at the ISNPS consists of a high-vacuum chamber and ion pump, a power rack, a control rack, PC-based data acquisition (CAMAC), and the Cs-Ba tacitron device. The chamber consists of a vacuum housing with a device mounting plate and electrical feed-throughs. There are 32 thermocouples channels, 12 high current insulated feed-throughs, 14 medium current channels for heaters, and 32 signal channels for control and measurement. The entire chamber is connected to a vacuum ion pump and enclosed in a water cooled jacket. The power rack contains the Cs and Ba reservoir heater regulators, the emitter and collector heater regulators, and the electrical supplies for the test stand. The control rack houses controls for all of the heaters, Cs and Ba reservoirs, electrical signals and data acquisition.

The diagnostic equipment consists of a CAMAC based multi-channel waveform digitizer for electrical measurements and an A/D converter for temperature measurements. In addition a D/A converter is used to send test signals for calibration of the current and voltage and to locate system errors. An IBM compatible 386-PC uses a GPIB interface to control the CAMAC. The test facility is demountable, hence many different electrode materials can be tested at various Cs-Ba vapor mixtures. The Cs and Ba reservoirs temperatures are independently controlled to adjust the vapor mixture pressure in the gap.

The Cs-Ba tacitron device currently being tested consists of two triode sections and one diode section. This configuration allows testing of not only the triode sections, but also the diode section, which basically is a thermionic converter. Figure 1 presents a schematic cross section and Table I lists the characteristic dimensions of the device. The emitter, grid and collector are constructed of molybdenum and the emitter heater is a 2 mm diameter tungsten rod surrounded by a tantalum tube. The tube returns the current from the tungsten heater to the power supply and prevents magnetic fields from developing due to the high heater current. Heating of the emitter is accomplished by thermal radiation from the tantalum tube or by electron bombardment, if a higher temperature is desired (>1800 K).



**1 - Cylindrical Molybdenum Emitter, 2 - Tungsten Heater,
 3 - Insulator, 4 - Grid, triode section 1, 5 - Collector, triode
 section 1, 6 - Collector, diode section 2, 7 - Grid, triode
 section 3, 8 - Collector, triode section 3, 9 - Barium
 reservoir connecting tube, 10 - Cesium reservoir,
 11 - Throttle apperture**

Figure 1. A Schematic Cross-Section of the Cs-Ba Tacitron

Table 1. Tacitron Physical Dimensions

EMITTER - MOLYBDENUM
Length: 44 mm
Inside Diameter: 8 mm
Outside Diameter: 16.5 mm
TRIODES
Collector - Molybdenum
Working Length: 7 mm
Inside Diameter: 25 mm
Outside Diameter: 70 mm
Grid - Molybdenum
Thickness: 1 mm
Aperture Diameter: 0.8 mm - 0.9 mm
Interelectrode Gap: 4.25 mm
Geometric Transparency: ~34%
Emitter-Grid Gap: ~1 mm
DIODE
Collector - Molybdenum
Working Length: 5 mm
Inside Diameter: 17.5 mm
Outside Diameter: 70 mm
Interelectrode Gap: 0.5 mm

Each triode section has a 1.0 mm thick grid, placed approximately 1.0 mm from the emitter surface. The three sections of the test device (see Fig. 1) allow testing of the diode section under the same operating conditions as the triodes. The temperature of the emitter is measured using three W-Re thermocouples mounted at different depths within the emitter (12 mm, 21 mm, and 37 mm, from the top of the emitter section), which correspond to the locations of the collectors in the three sections. The temperatures of the collectors, grid, Cs reservoir, and Ba reservoir are measured using type-K thermocouples. Type-K thermocouples are also used to monitor the temperatures in the different sections of the test facility. The following section presents some of the operation characteristics demonstrated in our facility and analysis and discussion of extinguishing results.

3. OPERATION CHARACTERISTICS

The tacitron test facility has been operational since January, 1991; test results are shown in Figs. 2, 4-12. Breakdown in the Cs-Ba tacitron, which usually occurs in the typical Paschen sense, can be altered by applying a potential bias to the grid. The pulse used to test breakdown is a half-sine wave with a constant DC offset and a peak voltage of 180 V. An example of a typical breakdown measurement for the tacitron is shown in Fig. 2 at the listed operating conditions. Following breakdown, 2.2 ms after applying the sinusoidal pulse, the collector voltage drops to about 10 V. However, the discharge current stabilizes at about 25 A, 2.5 ms after breakdown. Figure 2 also shows that during full discharge the grid current increases from zero to 4 A, which is limited by the grid power source. More details on the breakdown and ignition characteristics of the Cs-Ba tacitron as a function of the applied grid voltage are presented elsewhere.¹⁵ In this paper, the results on the parameters affecting the extinguishing characteristics, stable current modulation, low forward voltage drop and switching frequency are presented and discussed.

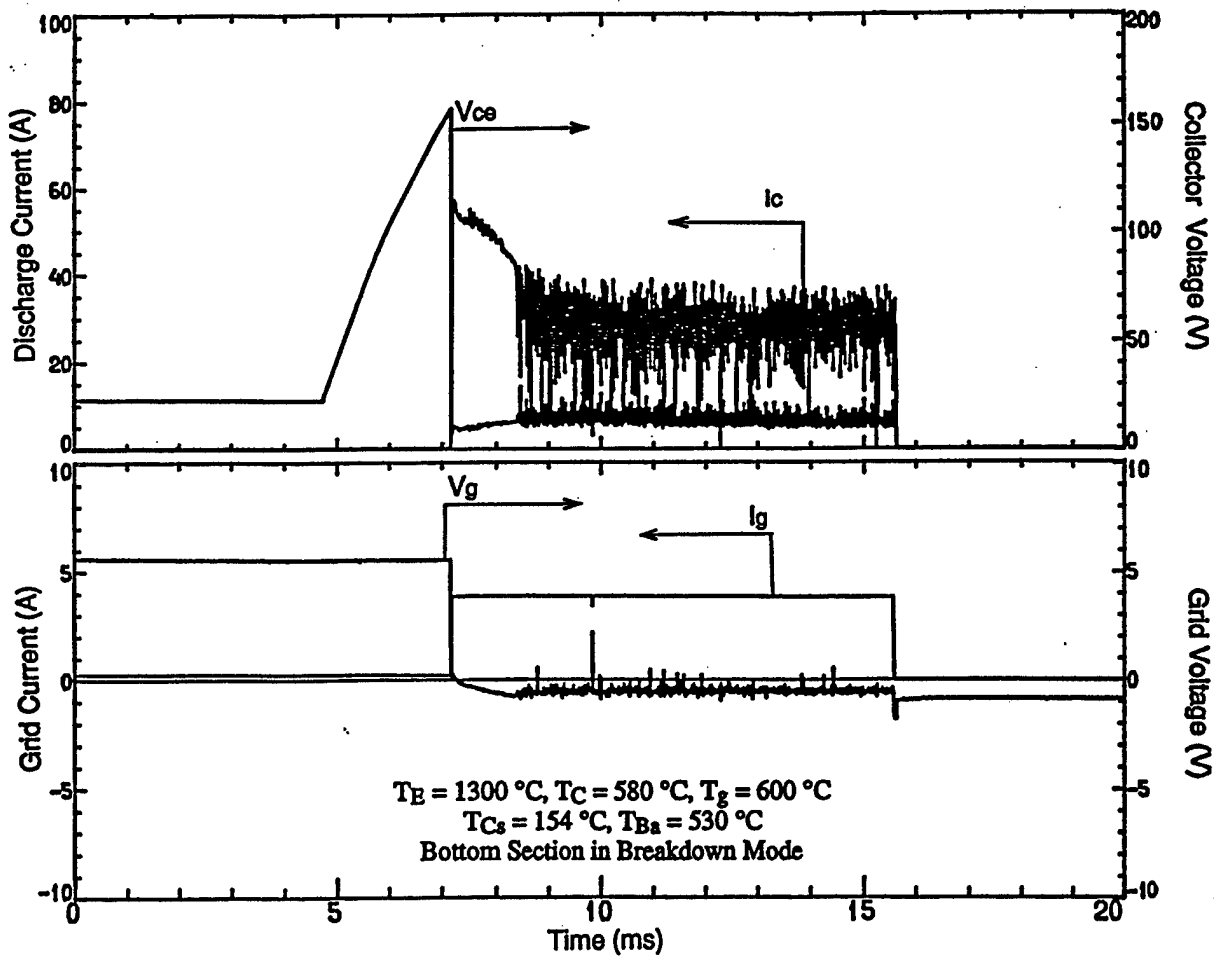
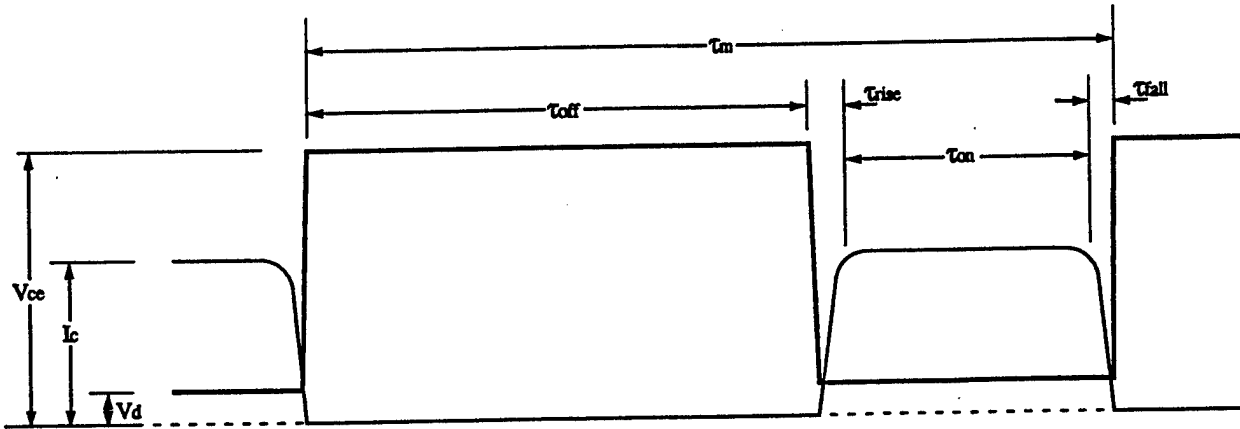
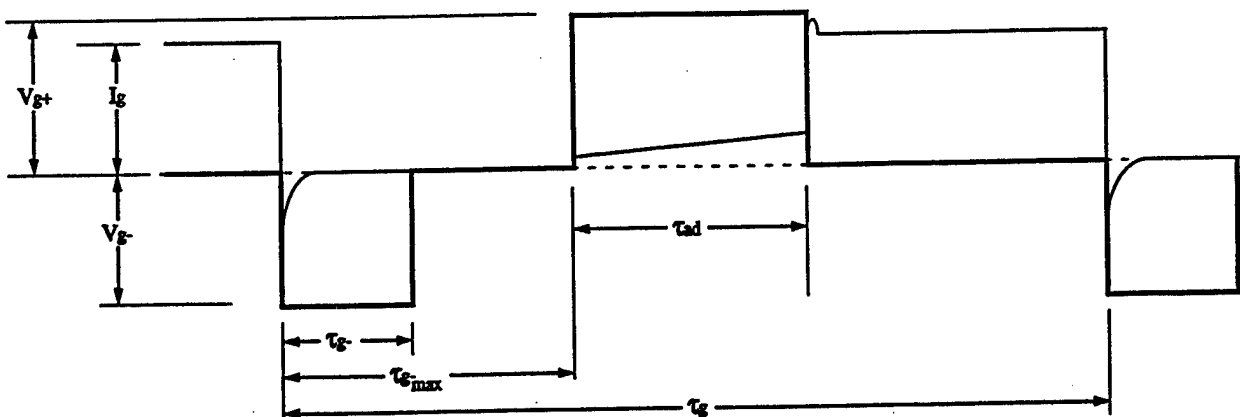


Figure 2. Typical Operation Characteristics of the Cs-Ba Tacitron in the Breakdown Mode



a) Typical collector voltage and current characteristics



b) Typical grid voltage and current characteristics

—	Voltage
—	Current
Stable Modulation Occurs when $\tau_m = \tau_g$	

Figure 3. Current Modulation Timing Diagram for the Cs-Ba Tacitron

3.1 Current Modulation Timing Characteristics

Before discussing the extinguishing characteristics of the tacitron, it is important to define the nomenclature associated with the different processes during current modulation. A typical timing diagram for stable modulation of the device is shown in Fig. 3. The upper part of the figure describes the collector voltage and current characteristics and the lower part of the figure describes the grid voltage and current characteristics. In each part, the darker (thicker) line represents the voltage and the lighter (thinner) line represents the current. Stable current modulation in the Cs-Ba tacitron occurs when the modulation frequency of the tacitron, f_m , equals the applied modulation frequency to the grid, f_g . Under this condition, the operating conditions (Cs pressure and discharge current) are such that discharge ignition and extinguishing occur when positive and negative pulses are applied to the grid, respectively. Failure to ignite and/or to extinguish the discharge results in unstable current modulation, causing f_m to be less than f_g . It is also possible to operate the tacitron in stable current modulation, but at different duty cycles, $(\tau_g - \tau_{off})/\tau_g$; thus operating at a different average power.¹⁵ The following sections show results representing both stable and unstable current modulation and values of the duty cycle during both modulation modes.

3.2 Extinguishing and Ignition Characteristics

The extinguishing and ignition characteristics of the bottom triode section at a frequency of about 5 kHz are shown in Fig. 4, the operating conditions are listed in the figure caption. The five regions of interest in Fig. 4 are labeled as: (a) off-state, (b) positive grid potential for ignition (c) ignition of discharge, (d) on-state, and (e) negative grid potential for extinguishing. Point (a) shows the off-state of the device with the collector potential, $V_{ce} = 140$ V, collector current, $I_c = 0$, grid current, $I_g = 0$, and grid voltage, $V_{g+} = 0$. At approximately 5.56 ms on the time scale a 22 V positive voltage for ignition is applied to the grid (V_{g+}), at which time the grid and collector currents increased gradually. The non square shape of the collector potential (see Fig. 4) is due to a 100 Ω resistor at the output of the collector voltage supply. This resistor is installed in order to determine the value of the collector current during the off-state from the measured voltage drop

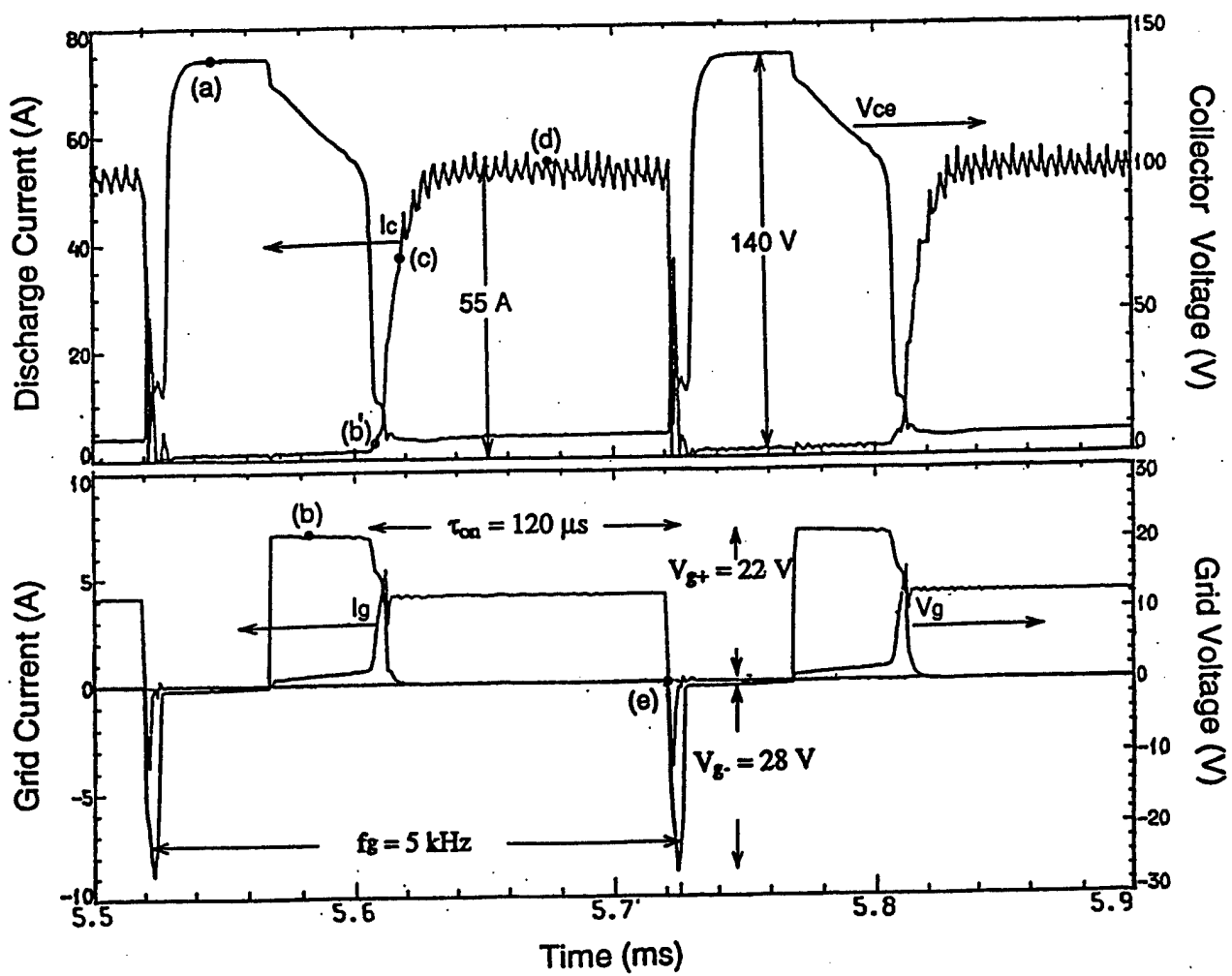


Figure 4. Extinguishing and Ignition Characteristics of the Cs-Ba Tacitron During Stable Current Modulation at 5 kHz ($T_E=1233$ °C, $T_C=583$ °C, $T_g=585$ °C, $T_{Cs}=151$ °C, $T_{Ba}=530$ °C)

across the resistor. At 40 μ s after applying the positive grid potential (τ_{ad}), a discharge develops between the emitter and grid. Shortly thereafter the main discharge ignites, point (b'), causing the collector and grid currents to increase, collector potential to decrease (voltage drop in the gap), and grid potential to drop to almost zero. As demonstrated in Fig. 4, full discharge is achieved after a 15 μ s rise-time (τ_{rise}), point (c). Full discharge, point (d), remains on until a negative potential, $V_{g-} = 28$ V, is applied to the grid, point (e). At this point, the induced instabilities interrupt the discharge. Eventually, the discharge is extinguished after a 5 μ s fall-time (τ_{fall}), resulting in $I_c = 0$, $V_{ce} = 140$ V and I_g going to zero. The 5 μ s fall-time is due to the oscillations in I_c and V_{ce} , prior to extinguishing (see Fig. 5). Figure 5 shows a blow up of the data collected during the current modulation conditions in Figure 4 at a sampling rate of 10^6 samples/sec. At point (a), the device is in the on-state (or full discharge) and at point (b) a negative pulse for extinguishing the discharge is applied to the grid, where the grid current becomes all ion current. At point (c), V_{ce} is the open circuit voltage, $I_c = 0$, $I_g = 0$ and $V_{g-} = 14$ V.

Although operating at a switching frequency of 5 kHz for a single triode is shown to be possible (see Figs. 4 and 5), the plasma behavior in the tacitron is not well understood. Sometimes, the main discharge is not ignited after applying a positive potential to the grid nor extinguished when a negative potential is applied to the grid (unstable modulation). Representative results of unstable modulation are shown in Figs. 6a and 6b. In Fig. 6a, because the time after extinguishing (off-time) is not long enough to replenish the Cs atoms, ignition does not occur when the positive grid voltage pulse is applied, but ignites when a second pulse is applied at a later time, point (a). After the second time the discharge is extinguished successfully, point (b), the discharge ignites at the end of the positive grid pulse, point (c). Shortly thereafter a negative potential is applied to the grid, but because the discharge has not been on long enough to reduce the amount of heavy components (mostly ions) in the discharge volume, the discharge did not extinguish. It is also seen in Fig. 6b, when the time after ignition is not long enough, the discharge fails to extinguish, point (a), but is extinguished when a second negative pulse is applied

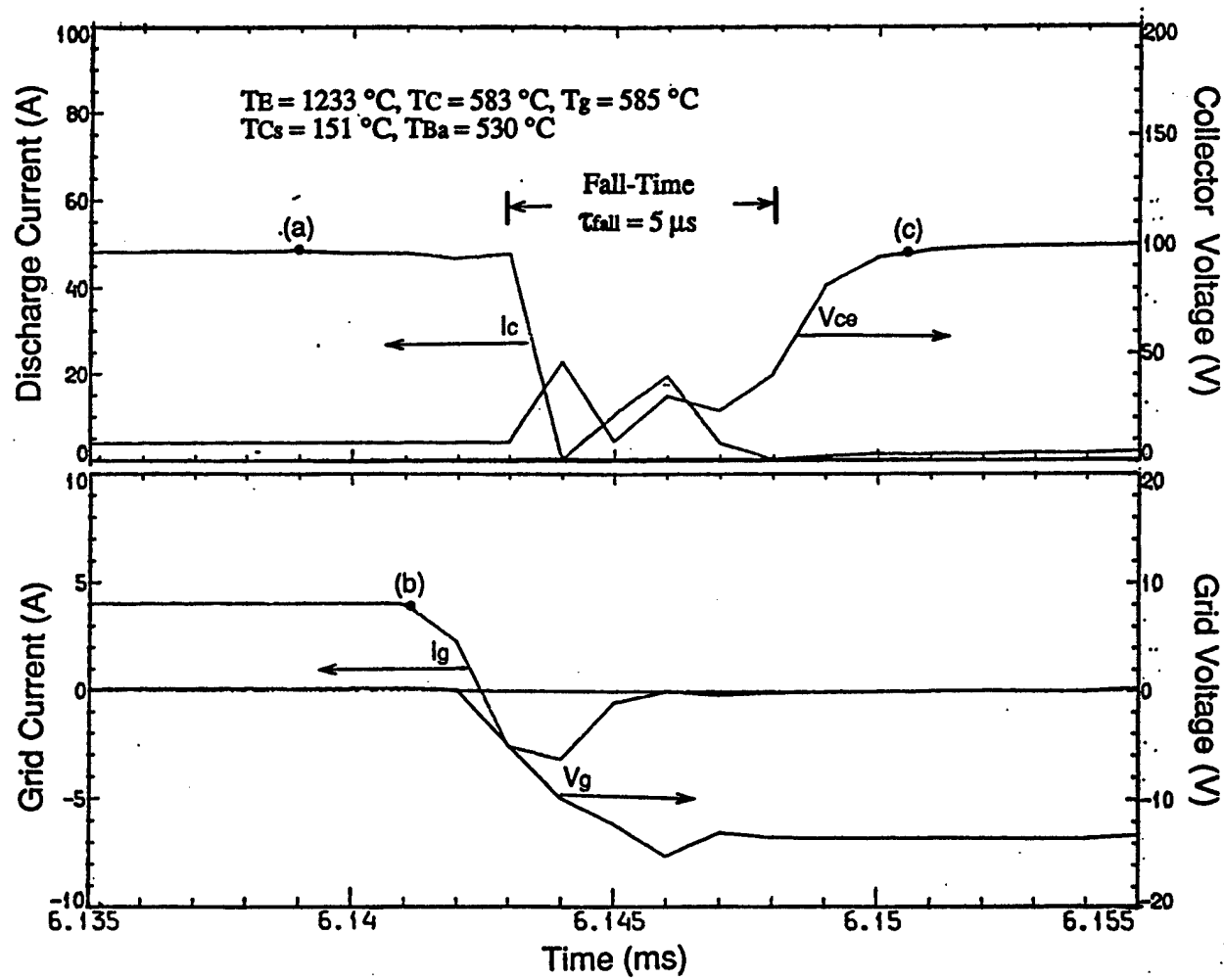


Figure 5. Voltage-Current Characteristics of the Cs-Ba Tacitron During Extinguishing Phase of Stable Modulation at 5 kHz

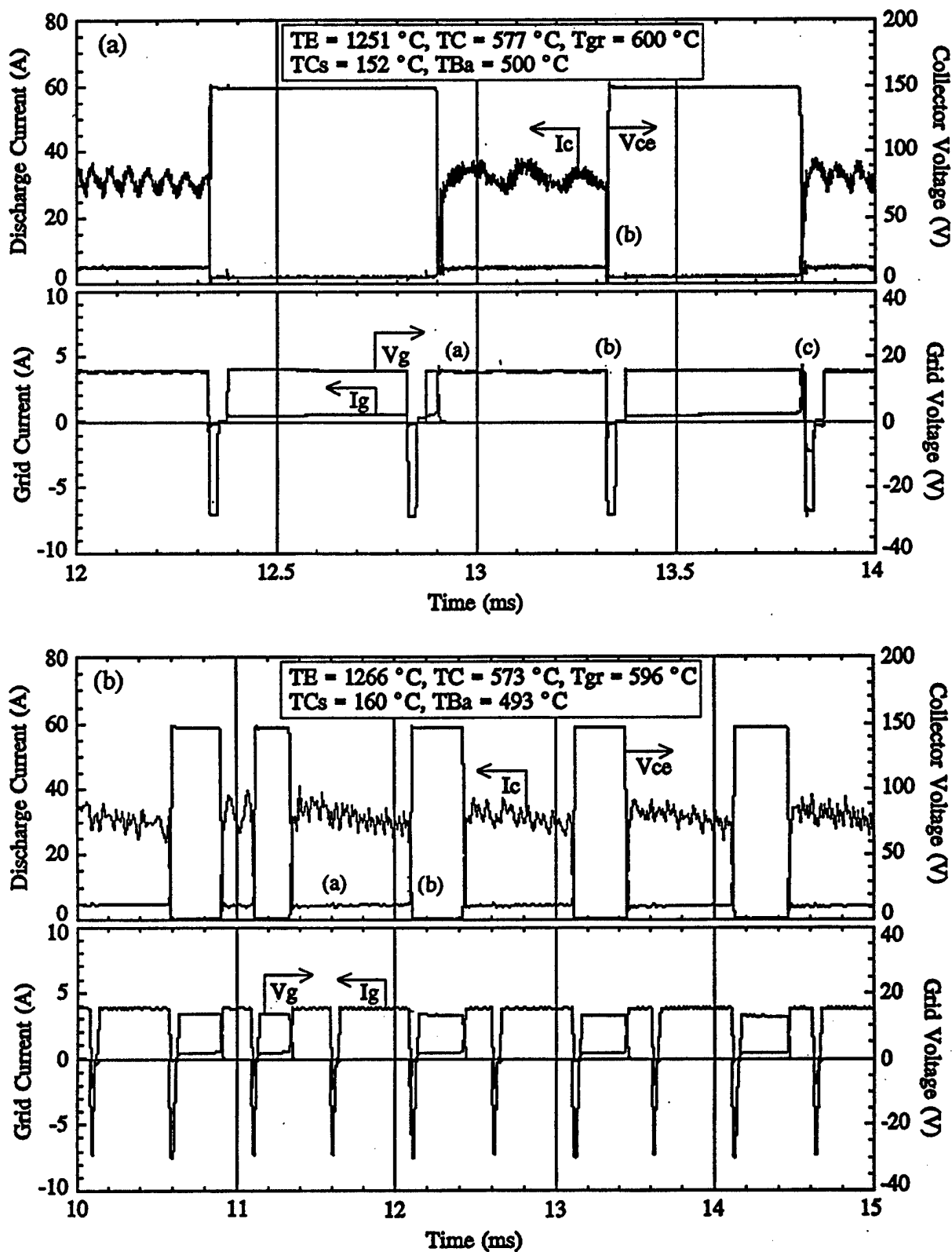


Figure 6. Typical Characteristics During Unstable Current Modulation of the Cs-Ba Tacitron; (a) failure to ignite during the positive pulse to the grid, (b) failure to extinguish during the negative pulse to the grid

2-4 ms later, point (b). Figure 6b also shows that there is always a delay time for ignition to occur after applying a positive pulse to the grid, τ_{ad} .

Although, the geometry of the grid in the present device is far from optimal with respect to current modulation and voltage drop in the device during discharge, the diameter of the grid holes of 0.8 mm is chosen to investigate the tacitron working regimes under conditions of abrupt extinguishing. When mostly ion current exists after the application of a negative pulse to the grid the dimension of the Langmuir layer, calculated from "3/2 law" under typical conditions of current modulation, is on the order of 10^{-3} to 2×10^{-3} cm. (The Debye length calculated from the mean plasma concentration determined from the ion current to the grid at the moment of extinguishing, assuming typical electron temperatures of 10^4 - 1.5×10^4 K, is on the same order). Because the dimension of the volume discharge region for interruption by Langmuir shielding is about two orders of magnitude smaller than the diameter of the grid apertures, the mechanism for quenching the discharge in the Cs-Ba tacitron is different; it is basically caused the loss of heavy components from the discharge volume during conduction. This process is investigated further in the next sections.

3.2.1 Establishing of Equilibrium Condition

Following ignition of a discharge, the time required for the concentration of heavy components in the interelectrode gap to reach equilibrium depends on: (a) the flux of Cs ions leaving the gap, (b) the flux of Cs atoms entering the gap, and (c) the amount of Cs atoms in the gap. The latter depends on the Cs vapor pressure in the gap immediately before ignition and the net adsorption of Cs atoms from the surfaces of the grid and collector (cold electrodes) during discharge. At a Cs vapor pressure of 10^{-2} torr ($T_{Cs} = 155$ °C), the Cs atom density, n_a , in the gap, when discharge is absent, is approximately 10^{14} atoms/cm³. The corresponding flux of Cs atoms in the gap is:

$$\Gamma_a = 1/4 n_a \bar{v}_a = 1.25 \times 10^{18} \text{ atoms/cm}^2 \text{s} . \quad (1)$$

In Eq. (1) the average atom velocity, \bar{v}_a , is given by:

$$\bar{v}_a = \sqrt{\frac{8kT_a}{\pi M_a}}, \quad (2)$$

During discharge, the flux of Cs atoms from the surrounding into the discharge region remains the same as when the discharge is absent (Eq. 1); however, the ion flux from discharge region to the surrounding can be expressed as:

$$\Gamma_i = 0.61 n_i \sqrt{\frac{kT_e}{M_i}}. \quad (3)$$

At equilibrium conditions for a highly ionized plasma fluxes (1) and (3) must be equal. Through the use of this equality, the equilibrium ion density can be calculated as follows:

$$n_i^{eq} = \frac{0.654 P_{Cs}}{\sqrt{T_a T_e}} \quad (4)$$

The ion density in the gap at any time during the discharge can also be determined from the measured ion current, I_i , to the grid when a short negative pulse is applied to the grid as:

$$n_i = \frac{1.64 \times 10^{-2} I_i}{q A_{gs} \sqrt{\frac{M_i}{kT_e}}}, \quad (5)$$

where A_{gs} is the surface area of the grid ($\sim 13 \text{ cm}^2$). In this mode, the grid serves as a probe for determining the plasma conditions in the gap. The comparison of the calculated and measured values at equilibrium condition (Eqs. 4 and 5) is discussed in a later section.

The time for reaching equilibrium conditions depends on the fluxes in Eqs. (1) and (3) and the total amount of Cs atoms leaving the gap during the discharge and can be represented as:

$$\tau_{eq} = \frac{\Delta N_a}{(\Gamma_i^{\text{mean}} - \Gamma_a)S} \quad (6)$$

3.3 Conditions for Stable Modulation

It is seen from the previous examples (Fig. 6) that it is necessary to fulfill a minimum of two conditions in order to maintain stable modulation. First, the discharge should be kept on for a definite time after ignition has occurred (on-time, τ_{on}) in order to successfully extinguish by a negative pulse to the grid. Secondly, ignition of the discharge occurs only with a definite delay time after applying the positive pulse on the grid (τ_{ad}). The on-time to extinguishing (τ_{on}) depends on the discharge current, I_c , electron temperature, T_e , and Cs vapor pressure. The delay-time for ignition (τ_{ad}) depends on the degree of decrease of the heavy component density in the gap during discharge, the magnitude of the positive voltage pulse to the grid and the Cs vapor pressure. During current modulation mode the Cs vapor pressure in the gap is lower than the surrounding regions. The Cs pressure in the gap decreases after ignition due to loss of heavy components into surrounding regions, and is restored after extinguishing due to the diffusion of Cs atoms from the surrounding regions. Therefore, the Cs vapor pressure in the discharge gap oscillates between two definite values at a frequency coinciding with the modulation frequency. Extinguishing and ignition are possible when these definite values of the Cs pressure are reached.

The relationship between the on-time and off-time for stable modulation can be expressed in terms of the duty cycle, η_d , where $\eta_d = (\tau_g - \tau_{off})/\tau_g$. In Figure 7, where regimes of stable modulation occur, the vertical axis shows the duty cycle, η_d , and the horizontal axis shows the positive grid voltage, V_{g+} . Data in Fig. 7 are measured at an applied grid modulation frequency of 2 kHz and a discharge current of ~ 45 A. This figure shows that for a given grid voltage pulse, increasing the initial Cs pressure increases the duty cycle of the tacitron. For example, at V_{g+} of 25 V, increasing the Cs pressure from 8.5 mtorr ($T_{Cs} = 150$ °C) to 13.5 mtorr ($T_{Cs} = 160$ °C) increases the duty cycle for stable modulation from 56 % to as much as 78 %. Therefore, the delay-time, τ_{ad} , is decreased and the time of the discharge is increased by increasing the positive

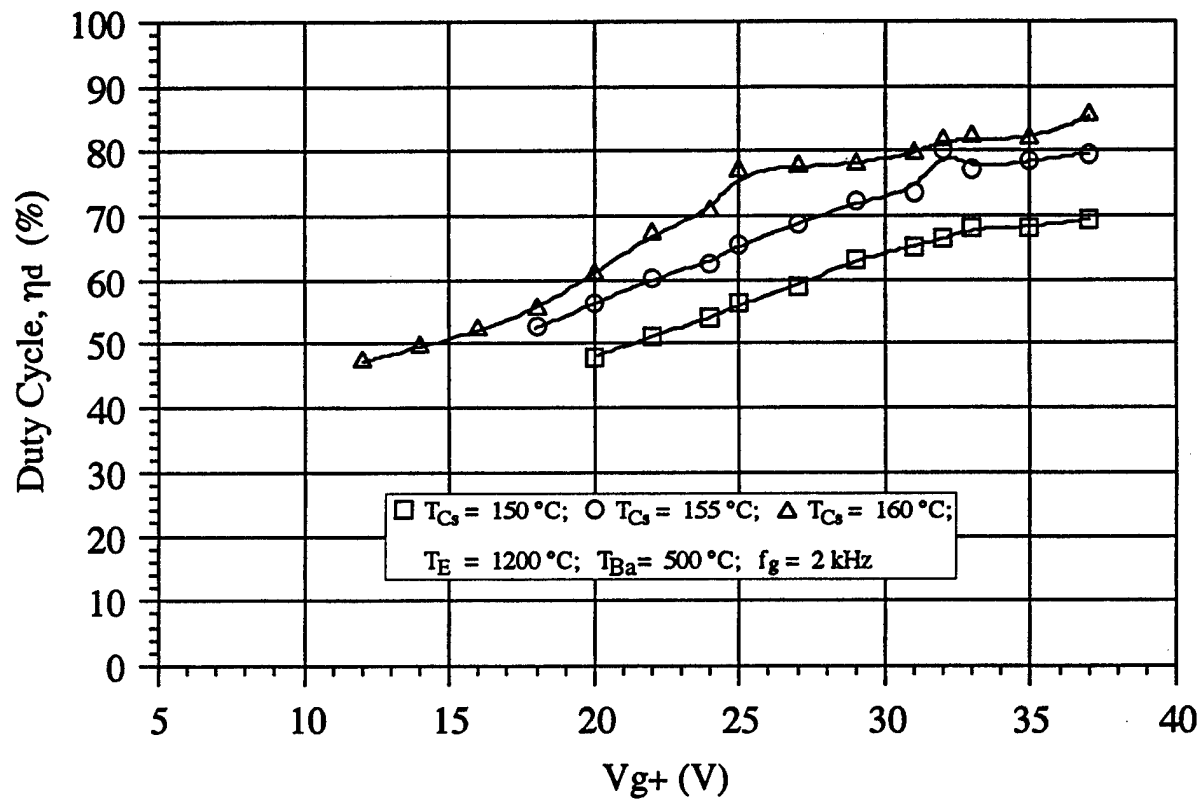


Figure 7. Duty Cycle as a Function of the Positive Grid Potential for Various Operating Parameters

grid voltage pulse for discharge ignition, which leads to increasing η_d automatically. These results are different at other modulation frequencies and discharge currents, but the general trend is that stable modulation for most regimes is seen at $\eta_d \simeq 50\%$.¹⁵ This similarity in behavior might be connected with equal variations in the values of the Cs vapor pressure in the gap corresponding to discharge ignition and extinguishing, respectively. This behavior is currently being investigated in more detail.

3.4 Forward Conduction Voltage Drop

The forward conduction voltage drop is an important parameter to future applications of the tacitron because it dictates the switching efficiency of the device and the range of input voltages that the device could be beneficial for. The switching efficiency, η_s , is defined herein as *the ratio of the difference between the applied open circuit voltage and the forward conduction voltage drop, ($V_{ce} - V_d$) to the applied open circuit voltage, V_{ce}* . In order to maintain a switching efficiency $>90\%$ for power systems having an output voltage as low as 50 V DC, the maximum voltage drop in the device should not exceed 4-5 V. Results to date show that at a given discharge current, the voltage drop in the triode sections decreases with increasing the Cs pressure in the gap and the emission current from the emitter. Because the Cs vapor pressure in the gap during current modulation is less than in the first moment of discharge ignition, the voltage drop, in the I-V mode, at the same discharge current, will be somewhat lower than that during current modulation at the same initial Cs pressure at the moment of the discharge. Therefore, it is interesting to analyze the change in the voltage drop with time during discharge ignition, I-V mode, as a function of emission conditions (T_E and T_{Ba}) and Cs pressure (T_{Cs}).

The changes in the discharge current and voltage drop with time after ignition in the I-V mode are shown in Figs. 8(a)-(e), 9(a)-(e), and 11(a)-(e), for different emitter temperatures and Ba and Cs vapor pressures. The source voltage used to generate the results in these figures is gradually

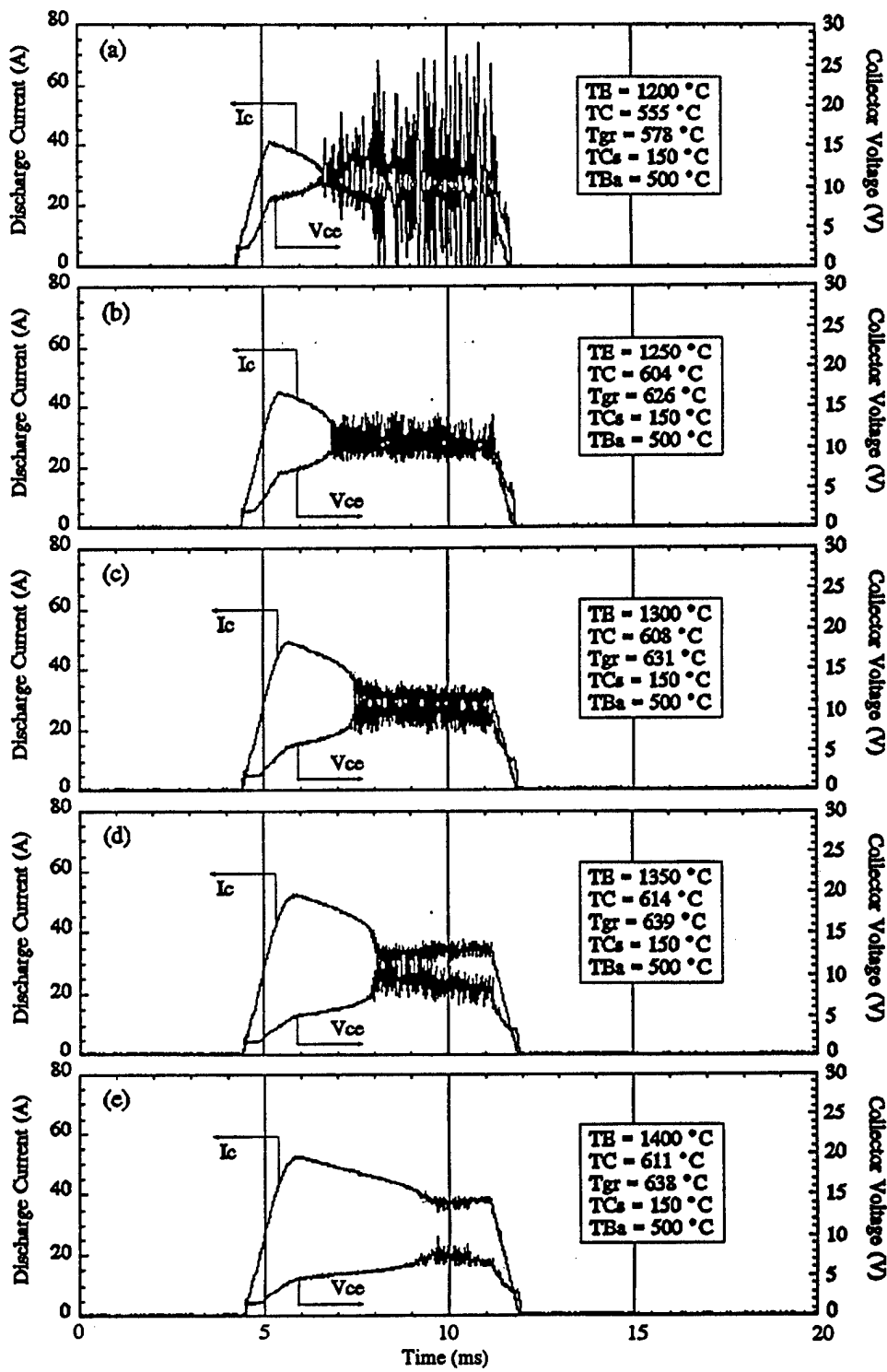


Figure 8. Time Response of the Discharge Current and Forward Voltage Drop Showing the Effect of the Emission Current at $T_{Ba}=500\text{ }^{\circ}\text{C}$ ($P_{Ba}=0.02\text{ mtorr}$) and $T_{Cs}=150\text{ }^{\circ}\text{C}$ ($P_{Cs}=8.5\text{ mtorr}$), (a) $T_E=1200\text{ }^{\circ}\text{C}$, (b) $T_E=1250\text{ }^{\circ}\text{C}$, (c) $T_E=1300\text{ }^{\circ}\text{C}$, (d) $T_E=1350\text{ }^{\circ}\text{C}$, and (e) $T_E=1400\text{ }^{\circ}\text{C}$

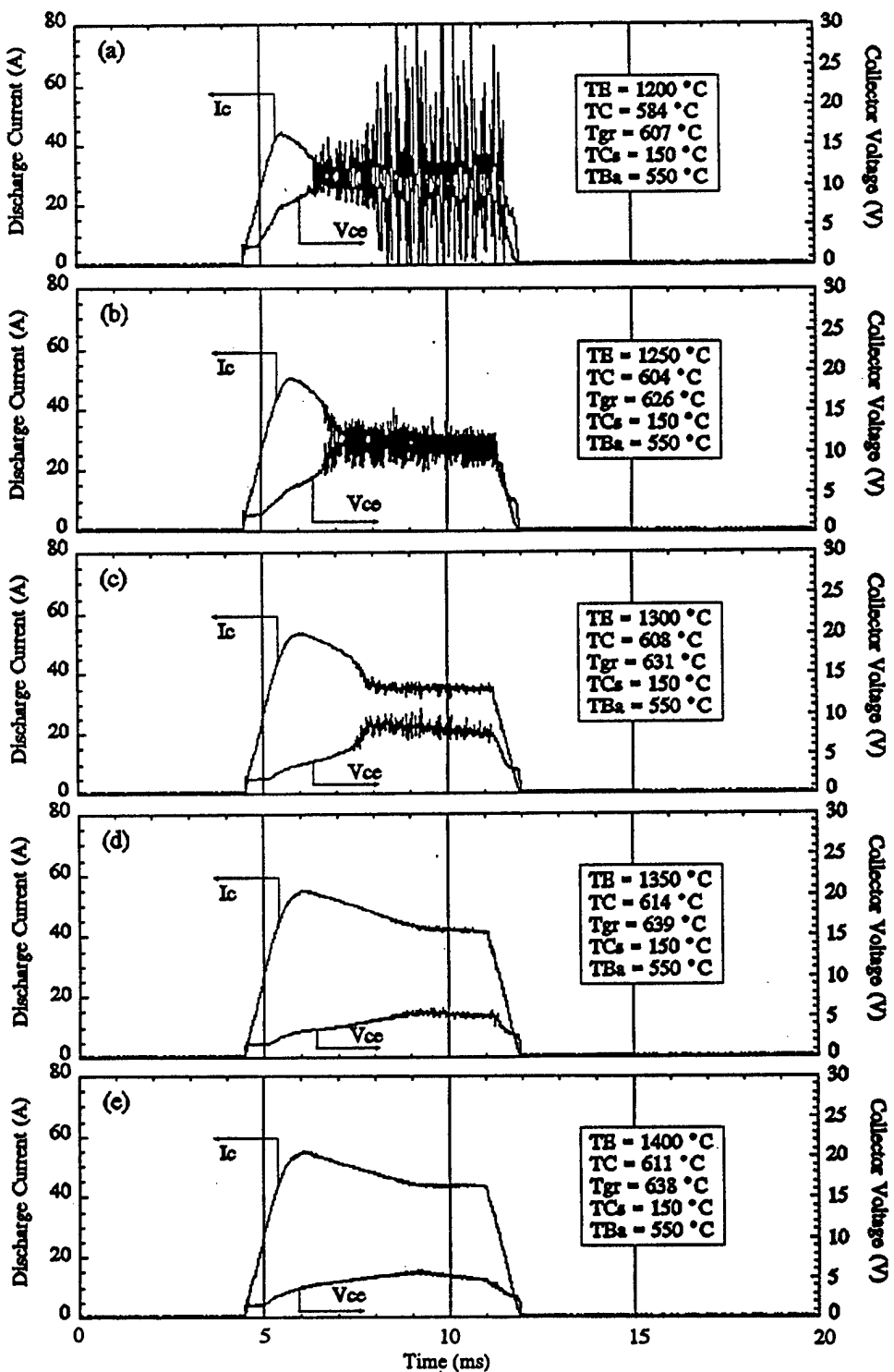


Figure 9. Time Response of the Discharge Current and Forward Voltage Drop Showing the Effect of the Emission Current at $T_{Ba}=550\text{ }^{\circ}\text{C}$ ($P_{Ba}=0.1$ mtorr) and $T_{Cs}=150\text{ }^{\circ}\text{C}$ ($P_{Cs}=8.5$ mtorr), (a) $T_E=1200\text{ }^{\circ}\text{C}$, (b) $T_E=1250\text{ }^{\circ}\text{C}$, (c) $T_E=1300\text{ }^{\circ}\text{C}$, (d) $T_E=1350\text{ }^{\circ}\text{C}$, and (e) $T_E=1400\text{ }^{\circ}\text{C}$

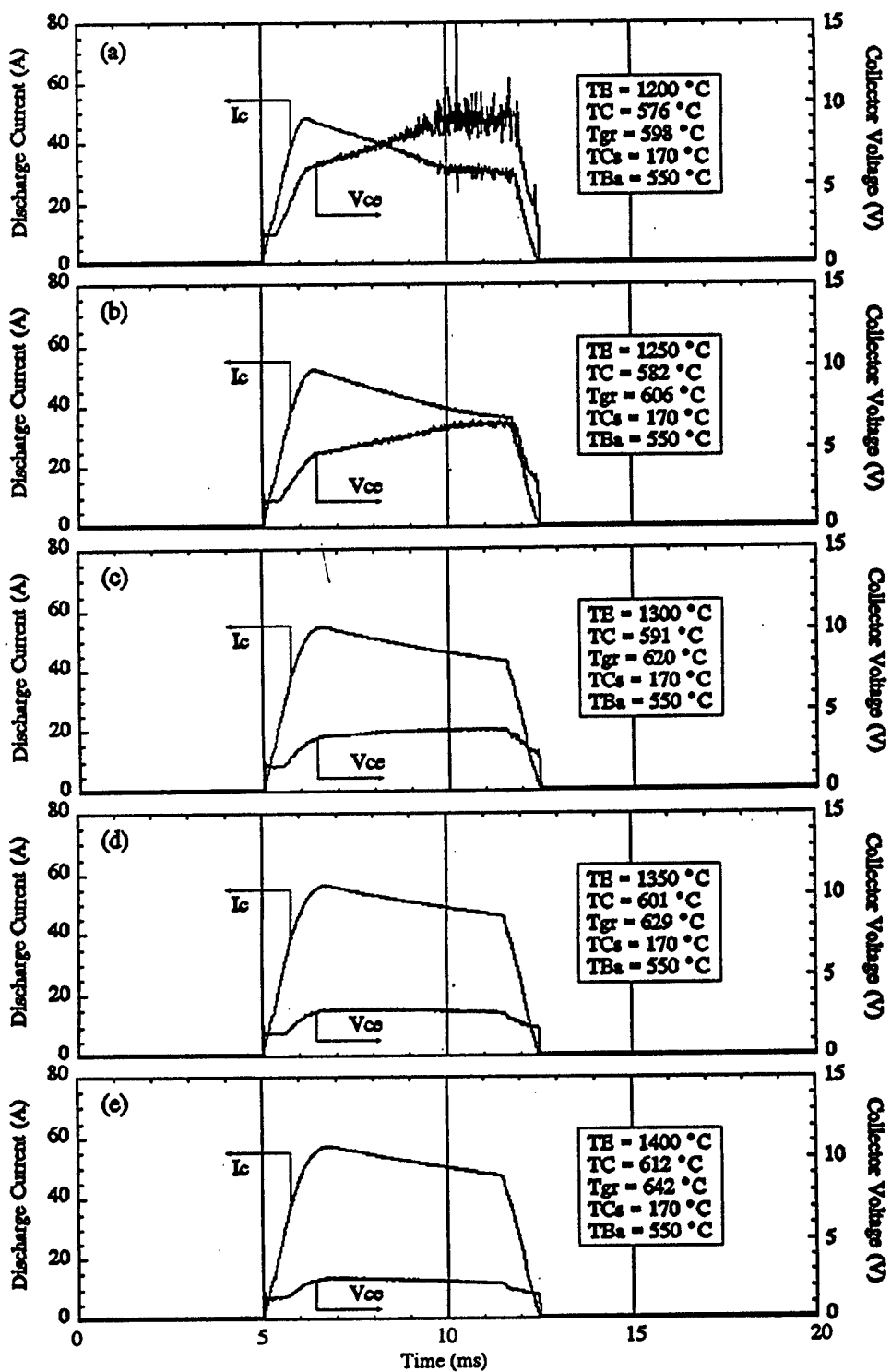


Figure 10. Time Response of the Discharge Current and Forward Voltage Drop Showing the Effect of the Emission Current at $T_{Ba}=550^\circ\text{C}$ ($P_{Ba}=0.1$ mtorr) and $T_{Cs}=170^\circ\text{C}$ ($P_{Cs}=21.4$ mtorr), (a) $T_E=1200^\circ\text{C}$, (b) $T_E=1250^\circ\text{C}$, (c) $T_E=1300^\circ\text{C}$, (d) $T_E=1350^\circ\text{C}$, and (e) $T_E=1400^\circ\text{C}$

increased up to 20 V during the first millisecond, and then it is maintained constant for the next 5 ms. During the subsequent millisecond the source voltage is gradually decreased from 20 V to 0 V.

In Figs. 8-10 the changes in the discharge current and voltage drop during the 5 ms period (starting at 6 ms on the time scale), when the source voltage is constant, is due to the decreasing Cs vapor pressure as a result of heavy components leaving the gap (i.e. ion current). As it is shown from the figures, the current rises initially at a practically constant voltage drop. At the end of the constant voltage drop region, at the point where the voltage drop begins to increase, the discharge current is practically equal to the emission current from the emitter. From the figures it is seen that this emission current increases with rising emitter temperature and/or Ba pressure. Further increase in the discharge current, causes the voltage drop to rise in order to increase the emission current partially by Schottky effect and partially by the increased ion current to the emitter. After the discharge current reaches its maximum value, it begins to decrease in spite of the increase in voltage drop. Such increase in the voltage drop occurs as a result of the decrease in the voltage drop on the external load as the discharge current decreases. The duration of decreasing discharge current, at the end of which equilibrium occurs, is related to non-stationary processes associated with heavy components leaving the discharge gap. As indicated earlier, such equilibrium is characterized by the equality of ion flux from the gap and the Cs atom flux into the gap. Results in Fig. 8 show that increasing the emission current, by increasing the emitter temperature, not only reduces the voltage drop, but also increases the discharge duration for reaching equilibrium (see Figs. (8a) and (8e)). For example, increasing the emitter temperature from 1200 °C to 1400 °C the voltage drop decreases from ~3.5 V to 2.5 V and the duration for reaching equilibrium increases from 3 ms to 4.5 ms.. Figure 8 also shows that the duration of the regions during which equilibrium is established increases as the emitter temperature is increased. As it is seen in Figs. 8-10, the duration of this equilibrium regime depends not only on the emitter emission but also on the Cs vapor pressure. Increasing the emitter emission (i.e. high T_E and/or P_{Ba}) and/or Cs vapor pressure increases the discharge time before equilibrium conditions in the gap and lowers the

corresponding voltage drop in the discharge region, which corresponds to increased voltage drop on the external load.

The low voltage drop is indicative of the lower energy dissipated in the plasma and therefore, the lower electron temperature, resulting in a lower ion flux from the gap (Eq. 3), which is proportional to the square root of the electron temperature. The low ion flux from the gap, increases the duration for establishing equilibrium (Eq. 6). In addition, increasing the Cs pressure, increases the amount of Cs atoms into the gap from the surrounding regions, hence increasing the time of reaching equilibrium in the gap. This effect is shown well in Figs. 8-10. The comparison of discharge current and corresponding voltage drop as a function of time at different emission conditions (T_E and/or T_{Ba}) testifies to the significant role the electron temperature has on the amount of heavy components leaving the gap during discharge. At a given Cs pressure (or T_{Cs}), the lower the emission and therefore discharge current, the larger the voltage drop and hence, the electron temperature, which affects the heavy component density in the gap, (refer to Eq. (4)). As Eq. (4) indicates, the heavy component density in the gap at equilibrium decreases as the electron temperature increases and/or the Cs vapor pressure decreases. The current and voltage oscillations in Figs. 8-10 at low emission (low emitter temperature and/or low Ba pressure) is indicative of the low heavy component density in the gap at high electron temperatures (Eq. 4). When the Cs vapor pressure in the surrounding space is increased, according to Eq. (4), the equilibrium ion density in the gap increases, causing the plasma oscillations in the discharge region to disappear (see Figs. 9(e) and 10).

The dependence of the discharge current and forward voltage drop in the discharge region at equilibrium conditions are shown in Figs. 11(a) and 11(b). The data delineated in Fig. 11 is taken at the point corresponding to 10 ms on the time scale in Figs. 8-10. The forward voltage drop values shown in Fig. 11(a), correspond to the discharge current in Fig. 11(b) at the same T_E/T_{Ba} . In Fig. 11(a) the forward voltage drop is not the lowest at the given emitter temperature, Ba and Cs vapor pressures, but rather that measured for a fixed external load and source voltage. It is possible to obtain a lower voltage drop at given T_E , P_{Cs} , P_{Ba} , and I_c by changing the external load. For

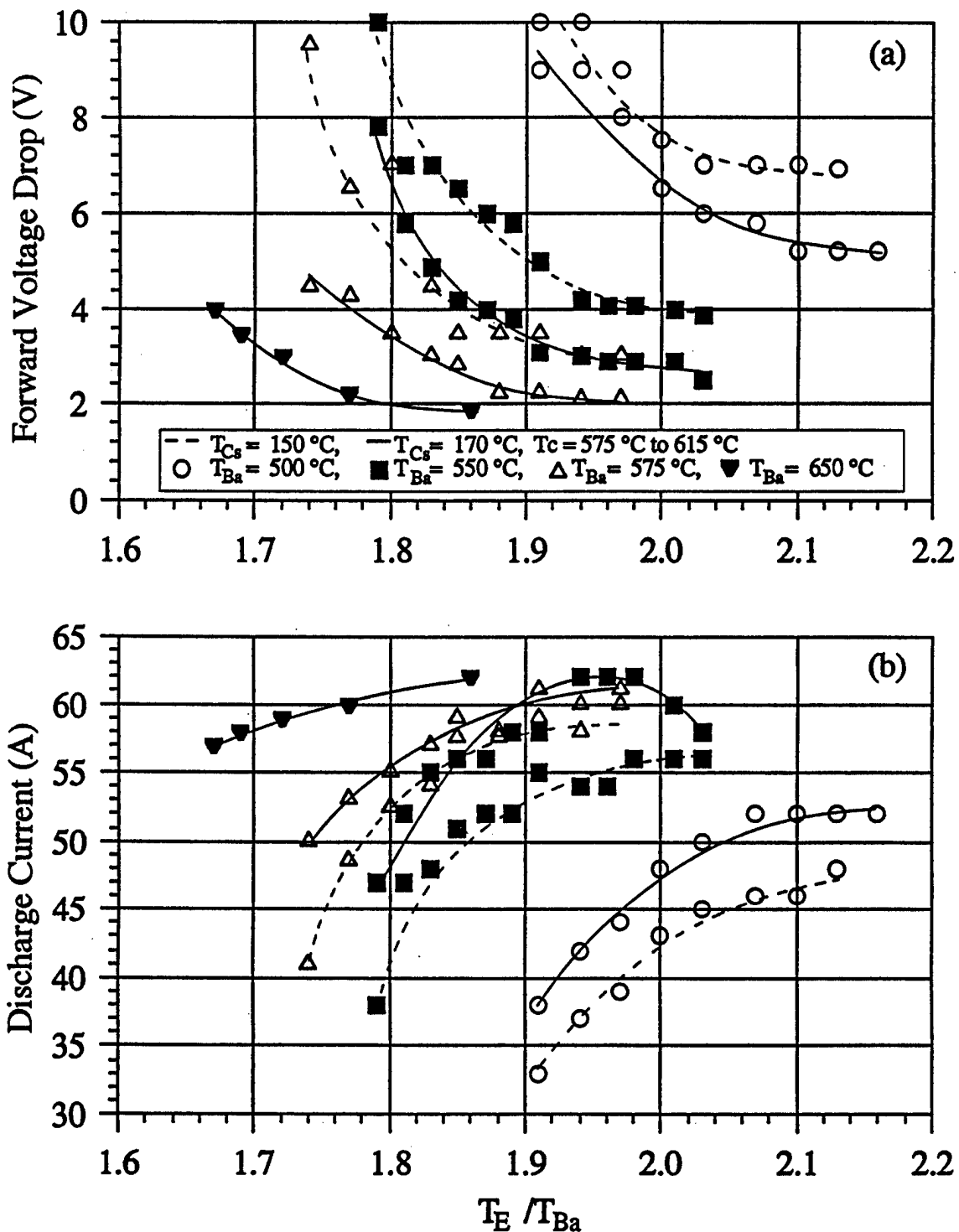


Figure 11. Effect of T_E/T_{Ba} ratio on the Discharge Current and Forward Voltage Drop of the Cs-Ba Tacitron, (a) forward voltage drop, (b) discharge current

example, at the beginning of the curves in Figs. 8-10 when the discharge current is not in excess of the emission current and the voltage drop is almost constant. Nevertheless, it is possible to evaluate the influence of emission current and Cs vapor pressure on the voltage drop utilizing the data in Figs. 11(a) and 11(b) and the data is based on Figs. 8-10. As these figures show, the voltage drop decreases as the Cs vapor pressure is increased.

Although the data in Fig. 11 is not directly applicable to current modulation mode, the effects of Cs pressure and emission conditions (T_E and P_{Ba}) on the voltage drop in the tacitron are expected to be similar. It is important to recognize that for a given grid geometry, stable current modulation is possible at definite combinations of the discharge current and Cs vapor pressure. In order to receive the lowest voltage drop, the discharge current, which can be controlled by the external load should be kept below the emission current; this is the region in Figs. 8-10 where the voltage drop is independent of the discharge current. The appropriate Cs vapor pressure is that resulting in highly ionized plasma in the discharge region at a given discharge current. For example, it is possible to reduce the voltage drop in the tacitron during stable current modulation from 6 - 8 V to 3 - 3.5 V by fulfilling the aforementioned two conditions, namely: (a) operating at a discharge current that is lower than the emission current, and (b) maintaining a Cs pressure that is high enough for ignition to occur when a positive pulse is applied to the grid but low enough to induce close to a fully ionized plasma in the discharge region so that when a negative pulse is applied to the grid, the discharge will extinguish. While the first condition reduces the voltage drop during discharge, the second condition should be fulfilled in order to maintain stable current modulation.

4. DISCUSSION AND ANALYSIS OF EXTINGUISHING RESULTS

The experimental results obtained for the Cs-Ba tacitron will indicate the time necessary for establishing equilibrium in the interelectrode gap during discharge and that for the onset of instabilities when a critical discharge current is approached. A series of single effect experiments are performed to illustrate the important parameters affecting the operation conditions of the device

during both stable current modulation, and breakdown modes. Also the effects of grid potential on the anode-delay time are investigated.

4.1 Unstable Modulation Regime

The time dependence of the measured discharge currents and forward conduction voltage when negative pulses are applied to the grid is shown in Fig. 12. The negative voltage pulses to the grid are utilized to probe the plasma and measure the ion current. This ion current is used to determine the mean plasma concentration in the discharge volume. Assuming an electron temperature, $T_e \approx 1.5 \times 10^4$ K, the equilibrium ion density obtained from Eq. (4) is $n_i = 2.2 \times 10^{13}$ cm $^{-3}$. As shown in Fig. 12, the measured ion current to the grid at the time of reaching equilibrium is about 3 A, for which $n_i = 2.45 \times 10^{13}$ cm $^{-3}$ according to Eq. (5). This value of the ion current is close to equilibrium as indicated by the very slow increase with time. Therefore, the conditions must be close to equilibrium. Indeed, the ion concentration calculated from the measured ion current to the grid at the time of extinguishing (2.45 $\times 10^{13}$ cm $^{-3}$) is very close to that calculated above assuming equilibrium and a highly ionized plasma in the interelectrode gap. However, this concentration is more than 3 times lower than that of Cs atoms at the initial Cs pressure of 10 $^{-2}$ torr before discharge is ignited. As shown in Fig. 12 the initial ion current after ignition is about 12 A, which corresponds to an ion density of 9.8 $\times 10^{13}$ cm $^{-3}$ using Eq. (5). This value coincides with the initial atom density of 10 14 cm $^{-3}$. Therefore, the plasma even at the first moment after igniting could be highly ionized

It is also possible to calculate the approximate time it takes for the discharge to reach equilibrium conditions from the measured ion current to the grid. As shown in Fig. 12, after the discharge is ignited, the ion flux to the grid decreases rapidly with time. The voltage pulses to the grid are applied continuously during the entire measurement time (~ 20 ms), although the pulses are plotted only during the first 2 ms in order to view the ion current. The clipped or constant portion of the grid ion current at the beginning of operation ($t=0$) is due to the limitation of the current by the grid pulse generator. The fact that the grid voltage during the constant portion of the

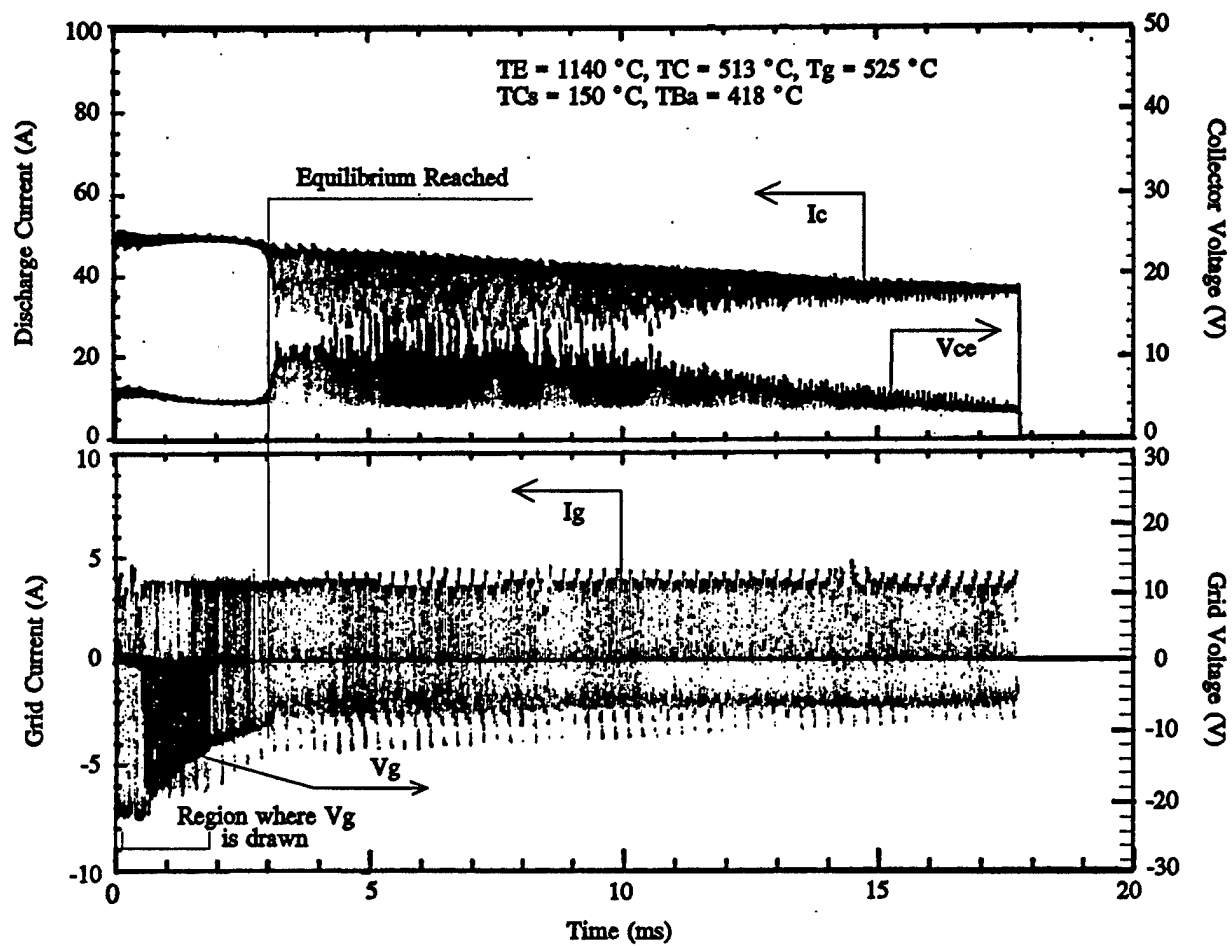


Figure 12. Discharge Current, Forward Voltage Drop and Ion Current to the Grid Illustrating Time to Reach Equilibrium During the Discharge.

grid current is almost zero, suggests that the ion current is being limited by the circuit. As Fig. 12 shows, while the ion current at the time of reaching equilibrium in the discharge is about 3 A, which corresponds to an ion flux of 1.44×10^{18} ion/cm²s, it could have been as much as 12 A at the time of ignition, which corresponds to an ion flux of 5.77×10^{18} ions/cm²s. These values give a mean ion flux during discharge, $\Gamma_i^{\text{mean}} = 3.51 \times 10^{18}$ ions/cm²s. Because this value is much higher than the Cs atom flux from the surrounding region into the gap, the average rate at which the heavy components in the gap decrease during the discharge period, τ_{on} , is equal to $(\Gamma_i^{\text{mean}} - \Gamma_a)$; this is on the order of 2.26×10^{18} particles/cm²s. If it is assumed that ΔN_a in Eq. (6) is the difference between the amount of heavy components in the volume of the gap before discharge ignition and during discharge after equilibrium is established, the following is received:

$$\Delta N_a = (n_{ao} - n_i^{\text{eq}}) V_{dr} \sim (10^{14} - 2.45 \times 10^{13} \text{ cm}^{-3}) 1.5 \text{ cm}^3 = 1.16 \times 10^{14} \text{ atoms}, \quad (7)$$

where V_{dr} is the volume of the discharge gap. Substituting this value of ΔN_a into (6) yields a characteristic time $\tau_{\text{eq}} = 100 \mu\text{s}$. As indicated in Fig. 12 and also in Fig. 13, this time is an order of magnitude lower than measured ($\sim 2 - 3 \text{ ms}$). Figure 13 shows the tacitron operating in the breakdown mode under similar conditions to those in Fig. 12. Therefore, the amount of atoms in the gap, immediately following discharge ignition, must have been significantly greater. The additional Cs atoms in the gap could have been provided by the desorption of Cs atoms from the electrode surfaces during discharge.

For a monolayer coating, the surface concentration of Cs atoms is about 2×10^{14} atoms/cm². Assuming no Cs atoms are present on the hot emitter surface, because of its low absorption capability to Cs in the presence of a barium film, and that the concentration of Cs atoms on the comparatively colder surfaces of the collector and grid decreases proportional to the reduction of the heavy component density, then:

$$\Delta N_a \sim (10^{14} - 2.45 \times 10^{13} \text{ atoms/cm}^3) 1.5 \text{ cm}^3 + (19 \text{ cm}^2 \times 1.25 \times 10^{14} \text{ atoms/cm}^2) = 2.5 \times 10^{15} \text{ atoms}$$

(8),

In Eq. (8) the first term accounts for the net change in the heavy components in the discharge volume, in the absence of Cs desorption, and the second term represents the contribution due to desorption of Cs atoms from the surface of the grid and collector during discharge. Substituting this value of ΔN_a in Eq. (6) increases the time to establish equilibrium during discharge, τ_{eq} , to ~ 2 ms, which is very close to the measured time of 2 - 3 ms in Figs. 12 and 13. Therefore, it is concluded that the source of Cs atoms in the gap, immediately following the initial ignition of the discharge ($t=0$), is not only the volume of the gap but also the desorption from the grid and collector surfaces.

4.2 Ignition Characteristics During Stable Modulation

During stable current modulation, especially at high frequencies, because the Cs atom concentration in the gap at the moment of applying the ignition pulse to the grid is significantly lower than that of the surrounding, ignition of the discharge is only possible after a certain delay time (see Fig. 14). This anode delay-time is needed to restore the Cs atom density in the gap. In Fig. 14, the operation in the modulation regime lowers the Cs atom concentration in the gap to the point where a positive grid voltage as high as 22 V would not cause instantaneous breakdown. When a high voltage pulse of 22 V is applied to the grid, small currents can be seen at the collector and the grid, which is an indication of ionization strengthening. In order to measure the low collector current before ignition, a 100Ω resistor is installed on the output of the collector power supply. At a stable source voltage, the collector potential decreases by the amount of voltage drop on this resistor, which is responsible for the linear decrease in the collector potential seen in Fig. 14. During the anode delay-time, τ_{ad} , before ignition occurs, the collector current is not only lower than that of the grid but its behavior lags it by 2-3 μ s. This delay-time coincides with the time it takes an ion to travel from the collector to the grid.

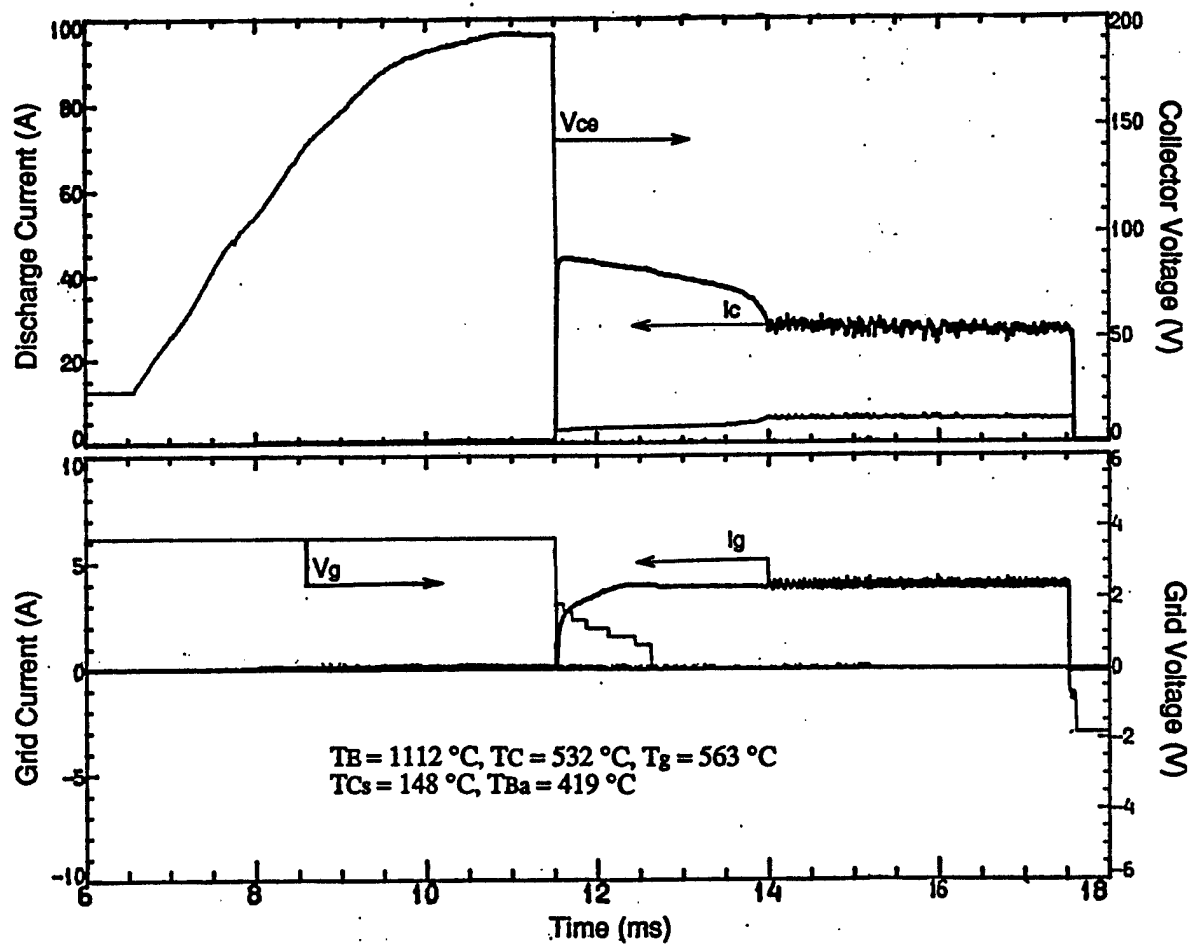


Figure 13. Discharge Current and Forward Voltage Drop Showing Time to Reach Equilibrium in the Breakdown Mode

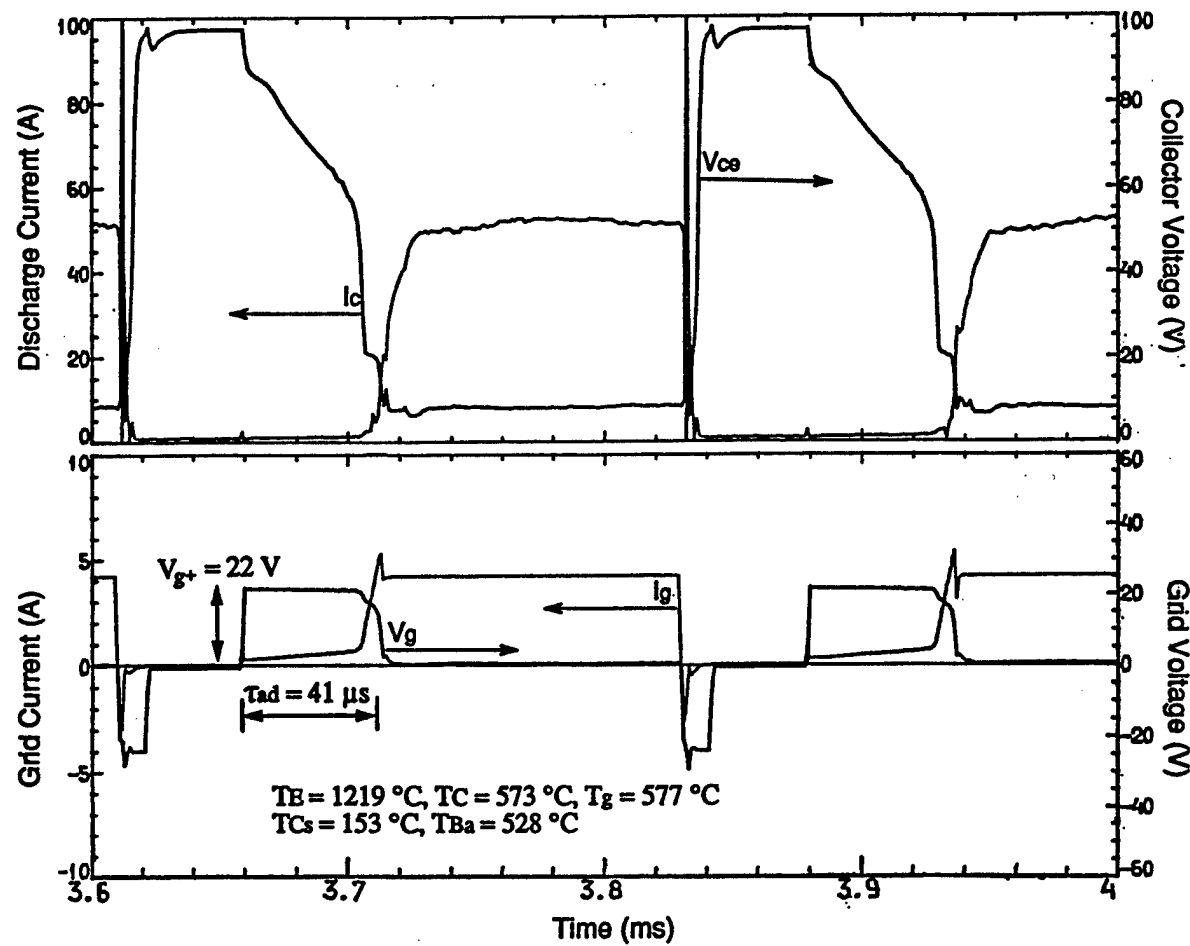


Figure 14. Stable Modulation of the Cs-Ba Tacitron Showing the Anode Delay-time for a Positive Grid Voltage of 22 V

As shown in Fig.15 (a), the discharge is ignited initially to the grid, and after a 2-3 μ s delay it propagates to the collector. The time interval between extinguishing the discharge and the application of the subsequent ignition pulse to the grid is 45 μ s. Figure 15(b) shows the collector current versus the voltage drop measured during the discharge advancement. In this case, there is an anode delay-time of about 50 μ s. The numbers next to the I-V characteristic data points give the time, in μ s, after the application of the ignition pulse to the grid. After igniting the discharge, the discharge current reaches a nominal level of 50 A after 16 μ s. The region with a negative resistance, lasting about 4 μ s (between 52 and 56 μ s), is indicative of the potential redistribution in the gap during the early phase of the discharge. The precipitous rise in the discharge current at 56 μ s reflects the spreading of the discharge along the electrode surface, which lasts about 12 μ s. Because this time is much longer than that expected to be associated with discharge formation it has to be connected with the induction of the outer leads. In Fig.15(b) the voltage drop at a current of about 50 A is about 6.5 to 7.5 V. This voltage drop is consistent with those shown in Figs. 8-10 at similar operating conditions (low T_E , P_{Cs} and P_{Ba}) 1.0 - 1.5 ms after ignition of the discharge in I-V mode. This higher voltage drop is due to the discharge current being larger than the emission current.

4.3 Effect of Grid Potential on the Anode Delay-time

The current modulation in Fig. 16 is for the same operating conditions as in Fig. 14, except at a higher amplitude of ignition pulses (30 V) for the grid. As shown in Fig. 16 the time between extinguishing the discharge and applying the subsequent ignition pulse is kept constant at 45 μ s. However, increasing the ignition pulse by 8 V (from 22 V to 30 V), shortens the anode delay-time from 50 μ s to 20 μ s; the rise-time to reach the nominal discharge current is about the same for both cases (18 μ s).

The effect of changing the time interval between extinguishing the discharge and subsequent application of the ignition pulse, at a modulation frequency of 7 kHz and comparatively low breakdown pulse amplitude of 22 V is illustrated in Fig. 17. As shown in Fig. 17, when the first

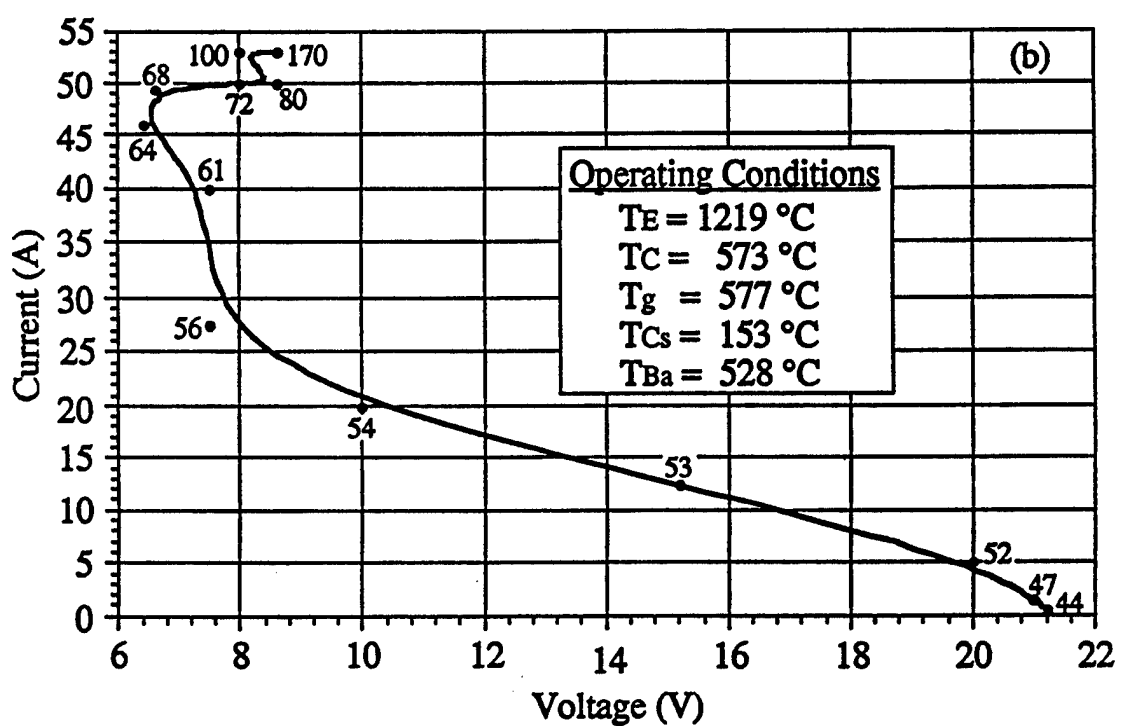
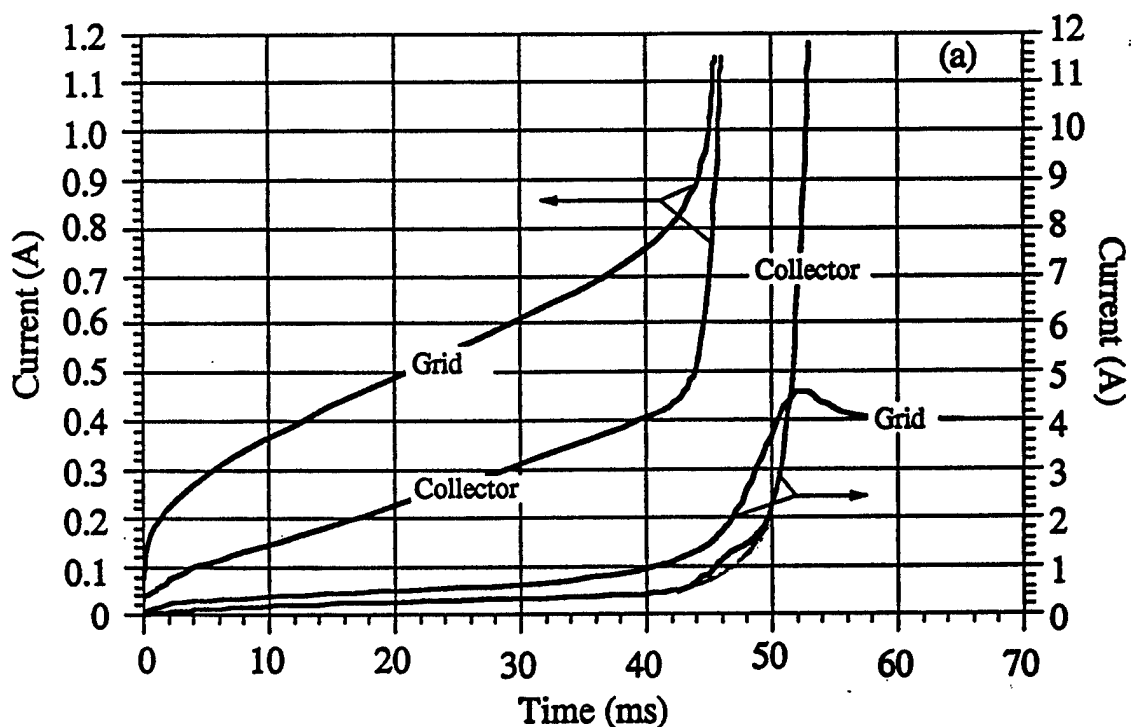


Figure 15. Time Dependent Voltage and Current Characteristics of the Cs-Ba Tacitron During Stable Modulation at $\sim 5\text{ kHz}$ and Positive Grid Potential of 22 V, (a) collector and grid current, (b) I-V characteristics. Operation conditions are the same as figure 14.

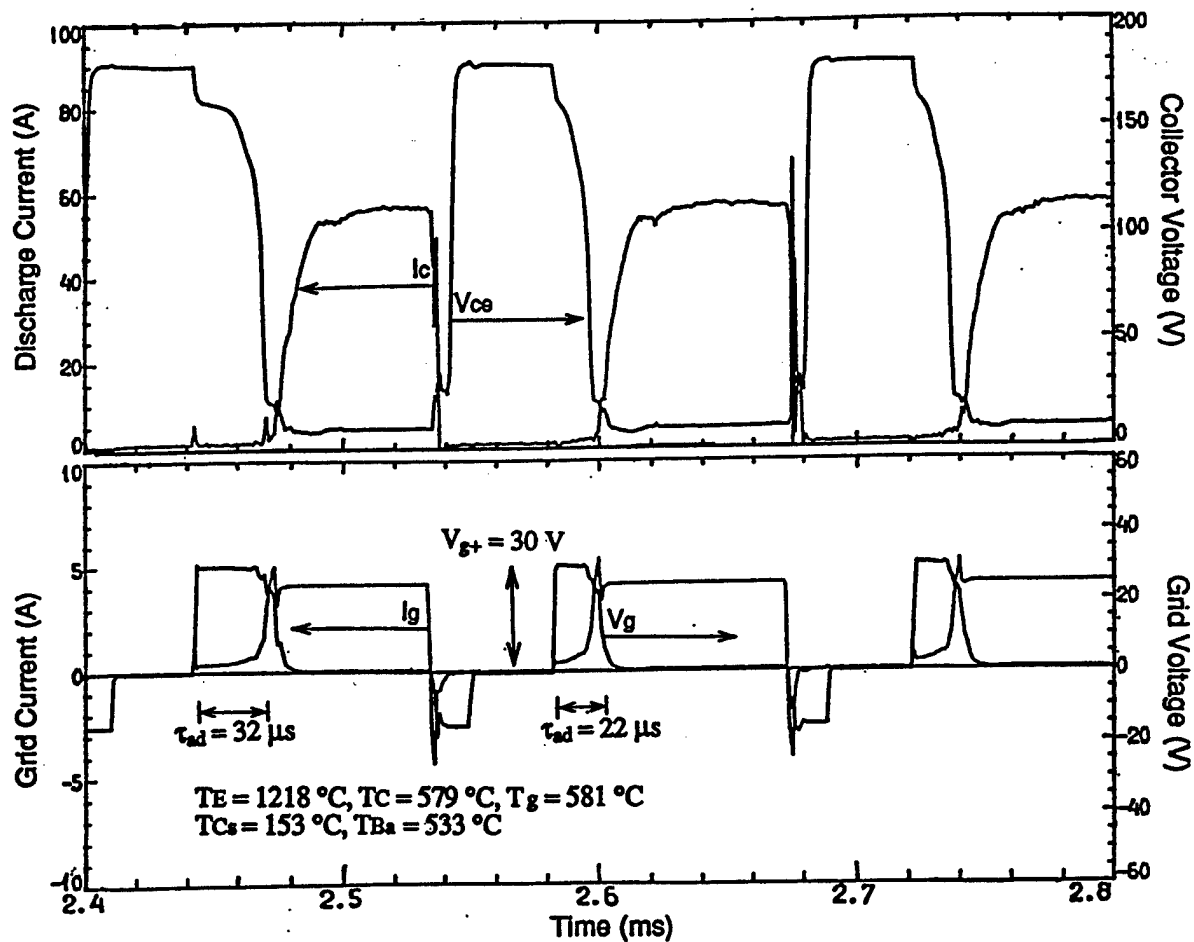


Figure 16. Effect of Increasing the Positive Grid Potential to 30 V on the Anode Delay-time During Stable Current Modulation

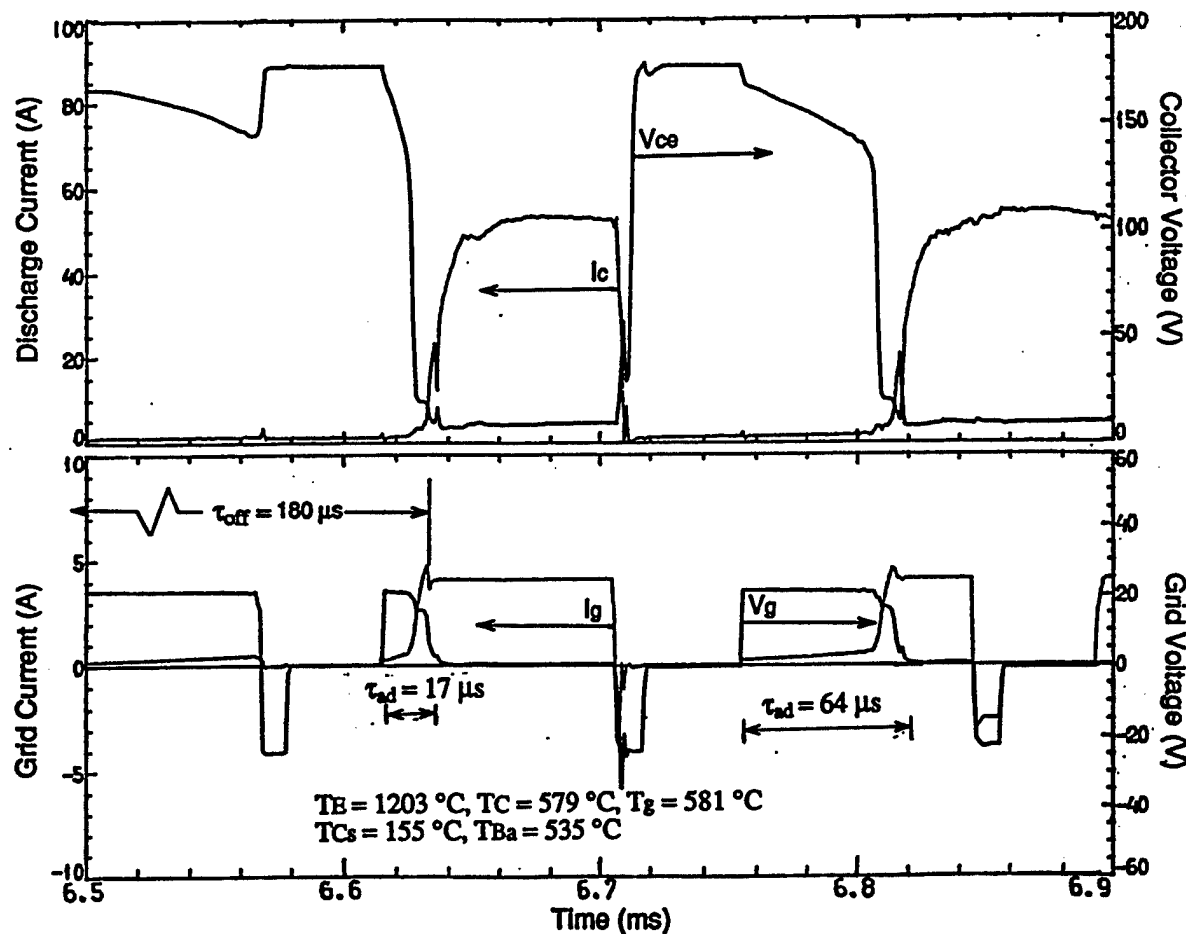


Figure 17. Effect of Increasing the Positive Grid Potential to 30 V on the Anode Delay-time During Stable Current Modulation

extinguishing pulse to the grid is applied, ignition did not occur, resulting in a total off-time of 180 μ s before the next ignition pulse to the grid is applied. During such time the Cs pressure in the gap increases, resulting in a short anode delay-time for the ensuing ignition (17 μ s). After extinguishing the second discharge, the off-time before applying the breakdown pulse decreased to 40 μ s and the anode delay-time increased to 60 μ s as shown in Fig. 17. However, the rise-time to reach the nominal discharge current of 45 A (about 15 μ s) is independent of the duration of the non-conducting state.

5. SUMMARY AND CONCLUSIONS

Experimental results demonstrate that the forward voltage drop in the Cs-Ba tacitron can be significantly reduced by increasing the emitter temperature, and the Ba and Cs partial pressures. Results show that for a Cs vapor pressure of ~20 mtorr, a Ba vapor pressure of ~0.1 mtorr, and an emitter temperature of 1670 K, the voltage drop in the top triode section, measured in I-V mode, can be as low as 1.5 V. But the voltage drop in current modulation mode can be different from that measured in I-V mode. It is necessary to keep in mind that, for a given grid geometry, stable current modulation is possible at definite combinations of the current density and Cs vapor pressure. In order to receive the minimum voltage drop, the discharge current should not exceed the emission current. The Cs vapor pressure is defined by the condition that the plasma in discharge would be close to fully ionized for a given discharge current. For example, the voltage drop in the tacitron during stable current modulation has been reduced from 6 - 8 V to 3 - 3.5 V by fulfilling the above conditions.

The important parameters influencing the different operation modes of the Cs-Ba tacitron are investigated. These modes include: (1) current modulation mode, (2) breakdown mode, and (3) the I-V mode. The effect of grid potential on the anode-delay time is also investigated. In the current modulation mode, the grid is used to probe the Cs ion density in the interelectrode gap during discharge. The ion density is determined from the measured grid ion current. Based on the agreement between analysis and measurements it is concluded that at the onset of instability,

leading to extinguishing the discharge, the plasma is highly ionized and that equilibrium exists between the ion flux leaving the gap and the Cs atom flux entering the gap.

The anode-delay time of the tacitron depends not only on the magnitude of the positive grid potential, but also on the length of the non-conducting state of the device. The delay-time before breakdown (time after applying the ignition pulse to the grid until the discharge ignites) of the Cs-Ba tacitron is reduced from 44 ms to 17 ms by increasing the grid voltage from 22 V to 30 V. The anode delay-time strongly depends on the length of the off-time. For example, when the off-time is increased from 40 ms to 180 ms, the corresponding anode delay-time decreases from 60 ms to as low as 17 ms. In general, stable modulation of the device during most regimes occurs at a duty cycle $\approx 50\%$; where increasing the Cs pressure increases the duty cycle beyond 50 %, as well as the value of the positive grid potential corresponding to the duty cycle threshold for stable modulation. These results may be different for other modulation frequencies and discharge currents.

ACKNOWLEDGEMENTS

The authors would like to thank A. Borovskikh, Y. Djashiashvili, and Y. Taldonov for the I.V. Kurchatov Institute of Atomic Energy, Moscow, Russia, for their help in the testing of the tacitron. We would also like to thank J. Freter from the Department of Chemical and Nuclear Engineering at the University of New Mexico, Albuquerque, NM, for his assistance in the processing of the data and preparation of the figures. Research sponsored by the Strategic Defense Initiative Organization and the Aero Propulsion and Power Directorate, Wright Laboratory, U. S. Air Force, Wright-Patterson AFB under Subcontract No. S-247-002-001, and by Idaho National Engineering Laboratory under Contract No. C89-102391 to University of New Mexico's Institute for Space Nuclear Power Studies.

REFERENCES

- 1 V. Z. Kaibyshev, G. A. Kuzin, and M. V. Mel'nikov, "Use of the Thermionic Converter for Regulation of Current in Electric Circuits", Soviet Physics Technical Physics, vol. 17, pp. 1006-1009 (1972).
- 2 V. Z. Kaibyshev and G. A. Kuzin, "Effect of a Third Electrode on a Low-Voltage Arc", Soviet Physics Technical Physics, vol. 20, 203, (1975).
- 3 Y. B. Kaplan, A. N. Makarov, A. M. Martsinovskii, A. V. Novikov, V. I. Serbin, B. I. Tsirkel, and V. G. Yur'ev, "Novel Low-Voltage High-Temperature Switching Element for DC-to-AC Conversion. I. Effect of a Grid on a Low-Voltage Cesium Arc", Soviet Physics Technical Physics, vol. 22, pp. 159-165 (1977).
- 4 V. Z. Kaibyshev, D. V. Karetnikov, and A. L. Trutnev, "Rectifying Parameters of a Thermionic-Emission Triode with an Auxiliary Discharge", Soviet Physics Technical Physics, vol. 23, pp. 1036-1039 (1978).
- 5 V. B. Kaplan, A. M. Martsinovskii, A. S. Mustafaev, V. I. Sitnov, A. Ya. Ender, and V. G. Yur'ev, "Spontaneous Current Cutoff in a High-Current Low-Pressure Cesium-Barium Discharge", Sov. Phys. Tech. Phys., vol. 24, pp. 325-328 (1979).
- 6 J. G. Andrews and J. E. Allen, "Theory of a Double Sheath Between Two Plasmas", Proc. Roy. Soc. Lond. A., vol. 320, pp. 459-472 (1971).
- 7 E. I. Lutsenko, N. D. Sereda, and L. M. Kontsevoi, "Investigation of Current Limitation in a Strong Current Discharge", Sov. Phys.-JETP, vol. 42, pp. 1050-1056 (1975).
- 8 O. R. Korendo, A. K. Musin, and S. F. Utenkova, "Low-Pressure Discharge in a Heterogeneous Medium", Sov. Phys. Tech. Phys., vol. 18, pp. 1061-1066 (1974).
- 9 I. Langmuir and H. Mott-Smith Jr., "Data on Discharge in Mercury Vapor Obtained with Cylindrical Collectors", Gen. Elect. Rev., vol. 27, pp. 762-771 (1924).
- 10 A. W. Hull and F. R. Elder, "The Cause of High Voltage Surges in Rectifier Circuits", J. Appl. Phys., vol. 13, pp. 372-383 (1942).

11 P.C. Standgeby and J.E. Allen, "Plasma State Current Amplifier", Nat. Phys. Sci., vol. 233, pp. 26-27 (1971).

12 V.Z. Kaibyshev, A. Borovskikh, Y. Djashiashvili, Y. Taldonov, M.S. El-Genk, C.S. Murray, and G.G. McDuff, "Peculiarities of the Discharge Breakdown of the Cs-Ba Tacitron", presented at the 2nd Annual Conference of Space Power, Sukumi, Georgia, USSR (October, 1991).

13 C.S. Murray, M.S. El-Genk and V.Z. Kaibyshev, "An Analysis of Extinguishing Characteristics of a Cs-Ba Tacitron", Proc. of the 9th Symposium on Space Nuclear Power Systems, Albuquerque, NM January 12-16 (1992), American Institute of Physics, Conf. Proc. No. 417, pp. 417-427 (1992).

14 M.S. El-Genk, C.S. Murray, S. Chaudhuri, V.Z. Kaibyshev, A. Borovskikh, Y. Djashiashvili, and Y. Taldonov, "Experimental Evaluation of Cs-Ba Thermionic Switch/Inverter - Tacitron", Proc. of the 26th IECEC Conference, American Nuclear Society, Boston, Massachusetts, vol. 3, pp. 160-165, (1991).

15 B. Wernsman, M.S. El-Genk and C.S. Murray, "Cs-Ba Tacitron: II. Ignition Characteristics During Breakdown and Current Modulation Modes", J. Appl. Phys. (companion paper submitted for consideration for publication, 1992).

16 A.A.W.M Garamoon and N.A. Surplice, "The Breakdown Potential and First Ionization Coefficient in a Townsend Discharge in Caesium Vapour", J. Phys. D: Appl. Phys., vol. 6, pp. 206-211 (1972).